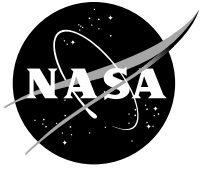


NASA/TM—2015-218891



# Particle Morphology and Elemental Composition of Smoke Generated by Overheating Common Spacecraft Materials

*Marit E. Meyer*  
*Glenn Research Center, Cleveland, Ohio*

---

December 2015

## NASA STI Program . . . in Profile

Since its founding, NASA has been dedicated to the advancement of aeronautics and space science. The NASA Scientific and Technical Information (STI) Program plays a key part in helping NASA maintain this important role.

The NASA STI Program operates under the auspices of the Agency Chief Information Officer. It collects, organizes, provides for archiving, and disseminates NASA's STI. The NASA STI Program provides access to the NASA Technical Report Server—Registered (NTRS Reg) and NASA Technical Report Server—Public (NTRS) thus providing one of the largest collections of aeronautical and space science STI in the world. Results are published in both non-NASA channels and by NASA in the NASA STI Report Series, which includes the following report types:

- TECHNICAL PUBLICATION. Reports of completed research or a major significant phase of research that present the results of NASA programs and include extensive data or theoretical analysis. Includes compilations of significant scientific and technical data and information deemed to be of continuing reference value. NASA counter-part of peer-reviewed formal professional papers, but has less stringent limitations on manuscript length and extent of graphic presentations.
- TECHNICAL MEMORANDUM. Scientific and technical findings that are preliminary or of specialized interest, e.g., “quick-release” reports, working papers, and bibliographies that contain minimal annotation. Does not contain extensive analysis.
- CONTRACTOR REPORT. Scientific and technical findings by NASA-sponsored contractors and grantees.
- CONFERENCE PUBLICATION. Collected papers from scientific and technical conferences, symposia, seminars, or other meetings sponsored or co-sponsored by NASA.
- SPECIAL PUBLICATION. Scientific, technical, or historical information from NASA programs, projects, and missions, often concerned with subjects having substantial public interest.
- TECHNICAL TRANSLATION. English-language translations of foreign scientific and technical material pertinent to NASA's mission.

For more information about the NASA STI program, see the following:

- Access the NASA STI program home page at <http://www.sti.nasa.gov>
- E-mail your question to [help@sti.nasa.gov](mailto:help@sti.nasa.gov)
- Fax your question to the NASA STI Information Desk at 757-864-6500
- Telephone the NASA STI Information Desk at 757-864-9658
- Write to:  
NASA STI Program  
Mail Stop 148  
NASA Langley Research Center  
Hampton, VA 23681-2199

NASA/TM—2015-218891



# Particle Morphology and Elemental Composition of Smoke Generated by Overheating Common Spacecraft Materials

*Marit E. Meyer*  
*Glenn Research Center, Cleveland, Ohio*

National Aeronautics and  
Space Administration

Glenn Research Center  
Cleveland, Ohio 44135

---

December 2015

## Acknowledgments

The author would like to gratefully acknowledge the microscopy performed by Victoria Bryg, SEM, High Resolution TEM and EDS (SEM) and Kristin Bunker and Traci Lersch of RJ Lee Group: High Resolution SEM/STEM Microscopy and EDS.

Trade names and trademarks are used in this report for identification only. Their usage does not constitute an official endorsement, either expressed or implied, by the National Aeronautics and Space Administration.

*Level of Review:* This material has been technically reviewed by technical management.

Available from

NASA STI Program  
Mail Stop 148  
NASA Langley Research Center  
Hampton, VA 23681-2199

National Technical Information Service  
5285 Port Royal Road  
Springfield, VA 22161  
703-605-6000

This report is available in electronic form at <http://www.sti.nasa.gov/> and <http://ntrs.nasa.gov/>

# Particle Morphology and Elemental Composition of Smoke Generated by Overheating Common Spacecraft Materials

Marit E. Meyer  
National Aeronautics and Space Administration  
Glenn Research Center  
Cleveland, Ohio 44135

## Abstract

Fire safety in the indoor spacecraft environment is concerned with a unique set of fuels which are designed to not combust. Unlike terrestrial flaming fires, which often can consume an abundance of wood, paper and cloth, spacecraft fires are expected to be generated from overheating electronics consisting of flame resistant materials. Therefore, NASA prioritizes fire characterization research for these fuels undergoing oxidative pyrolysis in order to improve spacecraft fire detector design. A thermal precipitator designed and built for spacecraft fire safety test campaigns at the NASA White Sands Test Facility (WSTF) successfully collected an abundance of smoke particles from oxidative pyrolysis. A thorough microscopic characterization has been performed for ten types of smoke from common spacecraft materials or mixed materials heated at multiple temperatures using the following techniques: SEM, TEM, high resolution TEM, high resolution STEM and EDS. Resulting smoke particle morphologies and elemental compositions have been observed which are consistent with known thermal decomposition mechanisms in the literature and chemical make-up of the spacecraft fuels. Some conclusions about particle formation mechanisms are explored based on images of the microstructure of Teflon smoke particles and tar ball-like particles from Nomex fabric smoke.

## 1.0 Introduction

Smoke particles were collected via a thermal precipitator (TP) during test campaigns at the NASA White Sands Test Facility (WSTF) (Meyer et al. 2013). A description of the device is given in NASA/TM—2015-218746 (Meyer 2015). Particles collected were subsequently examined with a Hitachi S-5500 scanning electron microscope (SEM), Hitachi HD-2300 scanning transmission electron microscope (STEM), and a Philips Model CM20 transmission electron microscope (TEM). The microscopes are equipped with energy dispersive X-ray spectroscopy (EDS) detectors that allow for elemental information of individual particles to be collected. Four potential substrates were incorporated into the collection surface for multiple microscopy options. A strip of conductive carbon tape was placed onto the surface of the SEM stub to allow for viewing of the particles on both the aluminum stub substrate as well as a neutral carbon background. TEM grids with a) continuous carbon film as well as a b) holey carbon film were placed at the edge of the carbon tape to allow sample collection for higher magnification examination. Smoke particle morphology gives insight into the thermal decomposition mechanisms of the spacecraft materials as well as the particle formation mechanisms, both important elements of smoke characterization. Elemental information on smoke particle composition gained from EDS provides additional information on individual particle characteristics. The polymeric fuel materials in this study had accompanying material data sheets, however, the specific formulations are proprietary and thus some additional constituents may be present such as plasticizers or colorants, which have the potential to affect the smoke production. Thus a number of elements are often observed in the EDS spectra which do not appear in the fuel chemical formula. In addition, there are other potential sources of elements, particularly Cu, Al and Si. The presence of Cu can be attributed to the TEM grid itself and a low Al peak may be

present owing to the sample holder of the microscope (therefore known as a system peak). The WSTF smoke generation process relies on a mica liner to hold the fuel during heating, which is another potential source of Si and Al in the smoke particles.

Thermal decomposition of the common spacecraft materials shown in this work mostly follow a common pattern. Under oxidative pyrolysis, a solid matrix of polymers will degrade and give off gaseous and liquid fuels which can be combined in high temperature reactions. These pyrolysis products are molecular fragments ranging in size from polymer chains down to the size of the monomer subunit of the polymer (Mulholland et al. 2015). Lower molecular weight materials can produce volatile species by evaporation or sublimation, whereas high molecular weight species which are cross-linked must undergo thermal decomposition at higher temperatures to produce gases. Polymers release low molecular weight gases upon initial heating followed by higher molecular weight pyrolysis products (Durlak et al. 1998). Saturated vapors emitted from the fuel either homogeneously nucleate into small molecular clusters as the gas cools, becoming internally homogeneous particles, or gases can condense onto existing particles which then appear as internally heterogeneous particles with inclusions or coatings. These formation mechanisms are distinctly different from soot formation in flaming combustion, which can be generalized into a three step formation mechanism consisting of 1) precursor species formation (when the complex fuel molecules are broken down into low molecular weight radicals which participate in many reactions), 2) particle inception (in which solid particle nuclei form and undergo surface growth by absorbing available gas phase molecules and becoming 20 to 24 nm spherules which agglomerate under Brownian motion in the flame), and finally 3) further agglomeration and surface growth, until the soot particle exits the flame when it cools and can potentially adsorb organic surface coatings (Moosmüller et al. 2009).

## **2.0 Overview of Heated Materials and Microscopy Results**

A summary of the SEM analyses performed using a field emission SEM (Hitachi S-5500) is given in Table 1 which describes the fuel, heating temperature, particle coverage obtained by the TP sampling, and qualitative descriptions of the particle sizes and morphologies observed. Two different thumbnail images are also provided in the table to show representative smoke particles from each sample at 5000x and 10,000x magnification. Images of smoke particles collected on the carbon tape have a somewhat bubbled texture in the background, most likely from the non-uniform adhesive under the carbon membrane. Images of smoke particles collected on the aluminum SEM stub surfaces often have a background pattern of faint parallel lines which are striations in the aluminum surface, as the stubs were not polished before use. Additional images and analyses from SEM, TEM, high resolution TEM and high resolution STEM are shown below for smoke particles from the following fuels: printed circuit board, wire insulation, Teflon, Kapton and Nomex.

Run numbers refer to the WSTF testing and can be cross-referenced to Meyer et al. 2013, where material descriptions and fuel preparation methods are outlined in detail. Wire insulation tests outlined here used PFPI insulation (partially fluorinated polyimide manufactured by TRW).

## **3.0 Smoke Particles From Printed Circuit Board Populated With Components**

A spacecraft fire could originate by overheating electronics, so circuit board materials are an important candidate for smoke characterization. As circuit boards are heated to above 250 °C, scission of high energy bonds takes place and small fragments are liberated along with monomers of the constituent materials. Above 500 °C, aromatic condensed ring systems (native to the original polymer or formed by reactions) will thermally decompose (Lambert, 1993).

TABLE 1.—SUMMARY OF SEM ANALYSES FOR WSTF FUELS

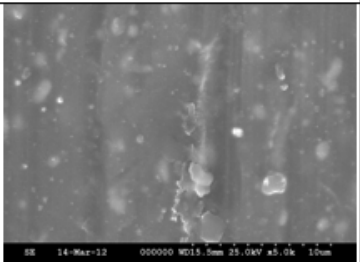
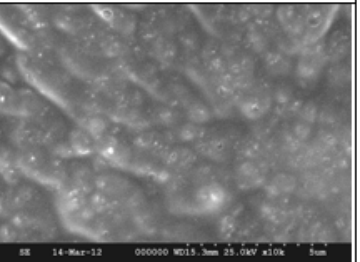
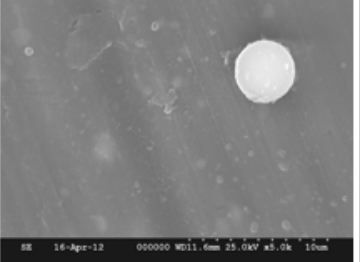
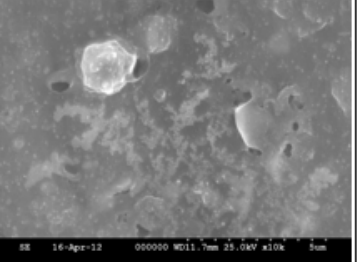
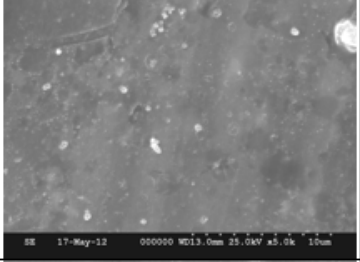
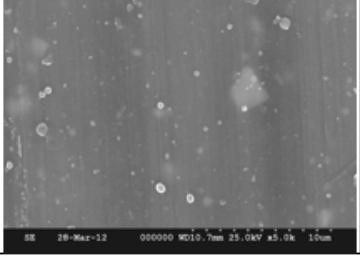
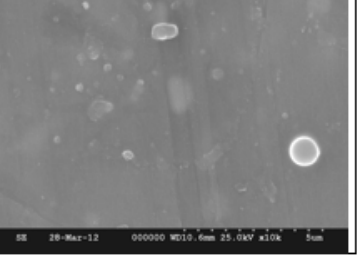
Run	Fuel	Temp/C	Particle coverage	Particle size (qualitative)	Particle Morphology	Image1 (5000X) <span style="float:right">10µm</span>	Image 2 (10,000X) <span style="float:right">5µm</span>
Run 3 & 35 Stub 2	Wire Insulation	540°	Sparse	Larger particles up to ~2.0µm; smaller particles generally ~0.1-~7µm.	Mostly spherical		
Run 6 Stub 2	Wire Insulation	640°	Fairly heavy	Generally ~0.2-5µm	Some large spherical particles, square crystalline particles, and individual particles as small as ~0.05µm.		
Run 29 Stub 2	Wire Insulation	640°	Sparse	Particles range from ~0.5 – 2.2µm. Most extremely tiny.	Most particles are spherical with those over 1.0µm appearing agglomerated; some droplet patterns visible.		
Run 8 Stub 2	Circuit Board	540°	Moderate	Most <2.2µm; most ~0.2-1.0µm.	Mostly spherical particles.		

TABLE 1.—CONTINUED.

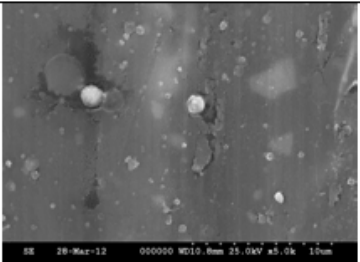
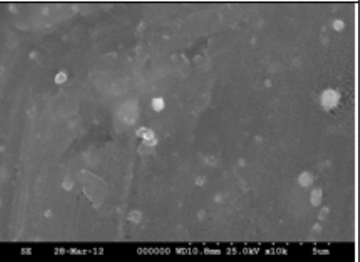
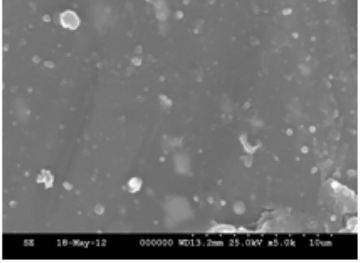
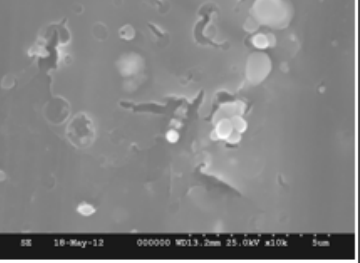
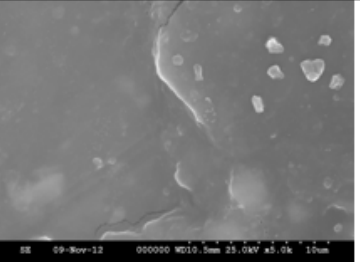
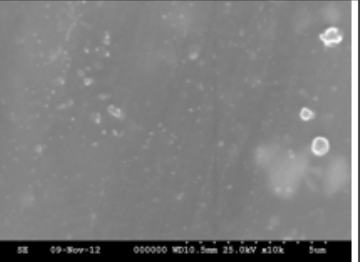
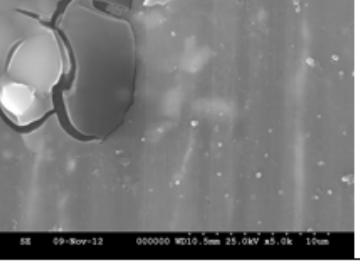
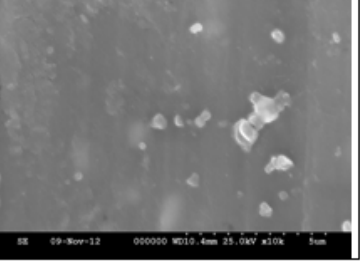
Run	Fuel	Temp/C	Particle coverage	Particle size (qualitative)	Particle Morphology	Image1 (5000X) 10µm	Image 2 (10,000X) 5µm
Run 23 Stub 2	Circuit Board	640°	Very heavy with film deposit	Many large agglomerates; most <2.2µm; most particles between 0.2µm and 1.2µm.	Many particulate agglomerates; particles mostly spherical; heavy textured deposit observed.		
Run 27 Stub 2	Circuit Board	340°	Film on stub surface with embedded particles	Generally range from ~0.2 – 2.2µm with many ~0.5-1.0µm	Particles generally spherical when sitting on smooth film; film appears broken in areas causing 'flakes'. Interesting salt containing droplet noted on Al.		
Run 30 (Sept)	Circuit Board	440°	Heavy	Particles usually <2.3µm. Smallest particles ~0.1-0.2µm.	Mostly a friable coating, with a few spherical particles.		
Run 33 (Sept)	Circuit Board	640°	Heavy	Large range of particles present, <0.1 to 12.6µm.	Heavy coating with most particles similar to Run 23.		

TABLE 1.—CONTINUED.

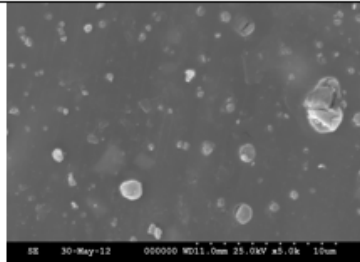
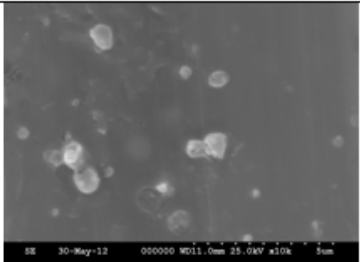
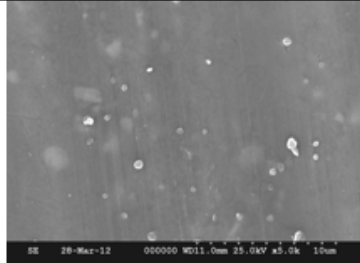
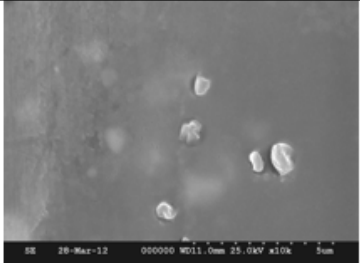
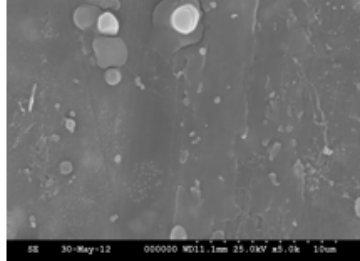
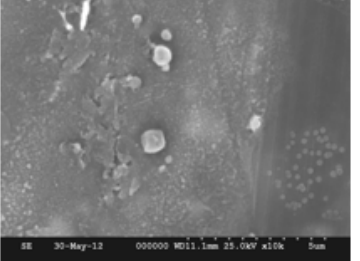
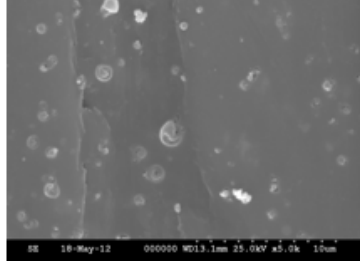
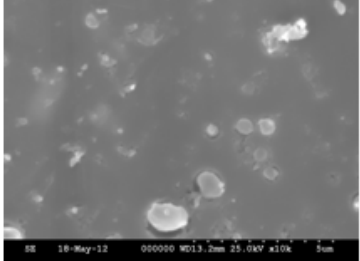
Run	Fuel	Temp/C	Particle coverage	Particle size (qualitative)	Particle Morphology	Image1 (5000X) 10µm	Image 2 (10,000X) 5µm
Run 9 Stub 2	100% TFE	540°	Heavy	Most particles <1.0µm, some up to 2.2µm.	Larger particles are somewhat spherical and agglomerated with primary particles measuring ~0.05-0.3µm.		
Run 15 Stub 2	100% TFE	640°	Moderate with film deposit	Most particles on Al stub <1.5µm; droplet on carbon tape ~5.0µm.	Many spherical particles along with thin needle-like crystals; crystals more easily observed on carbon tape.		
Run 42 Stub 2	100% TFE	640°	Moderate to heavy coverage with some droplet patterns visible.	Largest particles <3.3µm; generally 1-2µm, smallest ~0.2-0.3µm.	Smallest particles deposited in droplets; larger particles generally spherical and agglomerated.		
Run 36 Stub 2	90%/10% TFE/Kapton	640°	Fairly heavy	Particles range from ~0.1-1.6µm with many around 0.5-1.0µm.	Mostly spherical and 'compound' consisting of two different types of particles.		

TABLE 1.—CONTINUED.

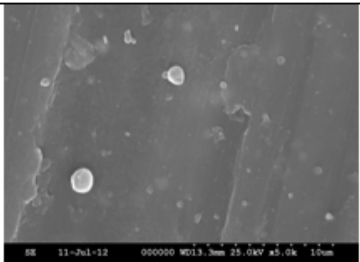
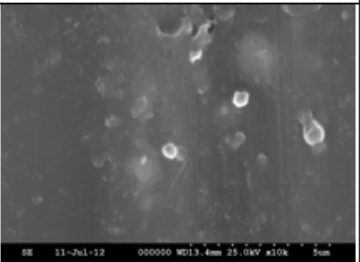
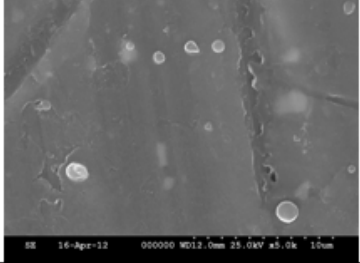
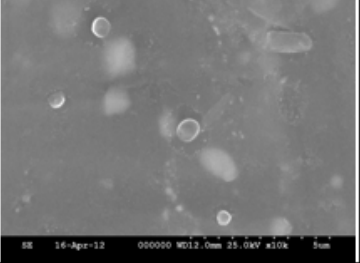
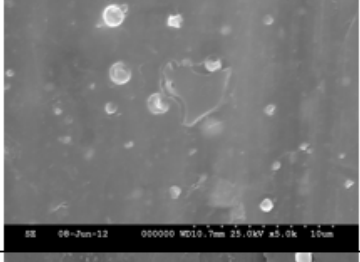
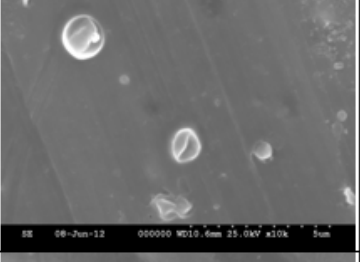
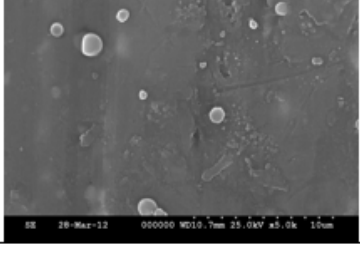
Run	Fuel	Temp/C	Particle coverage	Particle size (qualitative)	Particle Morphology	Image1 (5000X) 	Image 2 (10,000X) 
Run 14 Stub 2	75%/25% TFE/Kapton	540°	Sparse	Particles range in size from ~0.2µm-1.6µm; most appear to be <1.1µm.	Larger particles are somewhat spherical and appear to consist of two different types of particles.		
Run 19 Stub 2	75%/25% TFE/Kapton	640°	Film coated stub with individual embedded particles	Most ~0.2-2.2-µm.	Spherical particles with evidence of droplet patterns on substrate; smallest particles within droplets (~0.1µm).		
Run 12 Stub 2	50/50 TFE/Kapton	540°	Few particles, although beam damage indicates a coating on the stub.	Larger particles measure ~1-6.6µm; smaller particles are ~0.1-1.0µm.	Larger spherical particles are usually agglomerates mostly of similar size, sometimes various sizes; significant beam damage evident.		
Run 17 & 25 Stub 2	50/50 TFE/Kapton	640°	Heavy coverage over a film.	Spherical particles generally <2.5µm; agglomerated smalls ~0.1µm.	Thick deposits along with spherical particles; some inorganic particles noted; collapsed particles seen on carbon tape.		

TABLE 1.—CONTINUED.

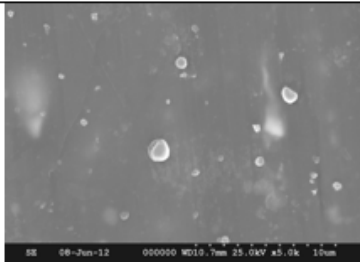
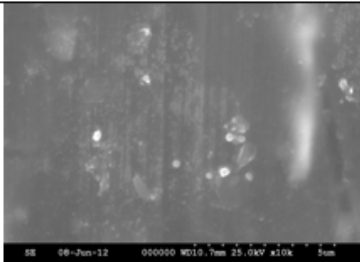
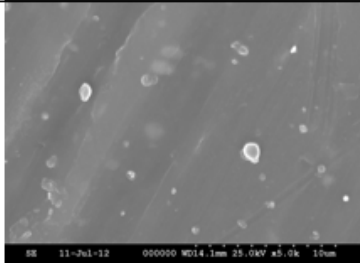
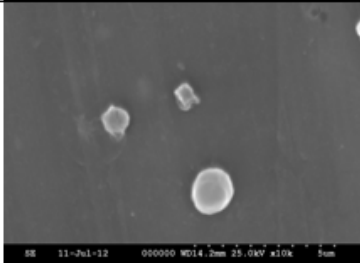
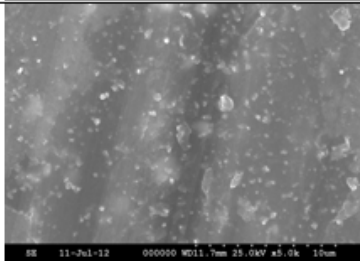
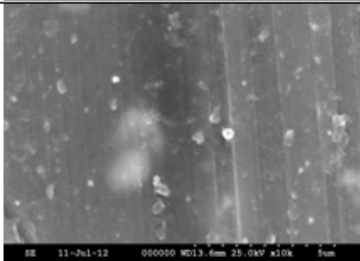
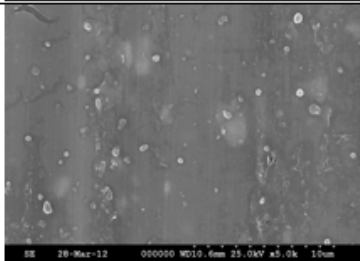
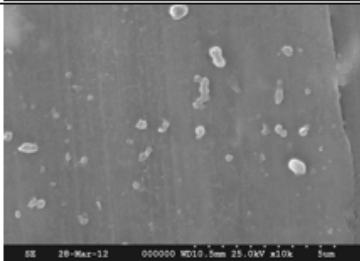
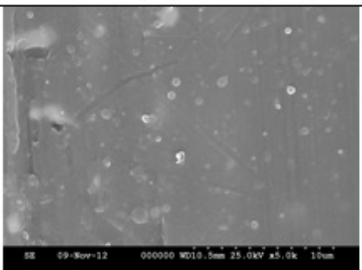
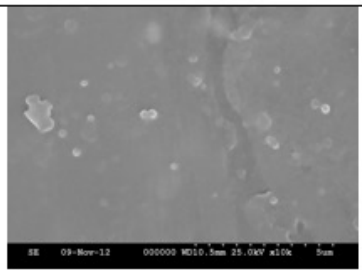
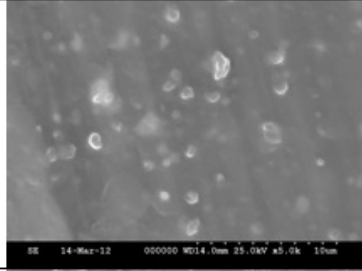
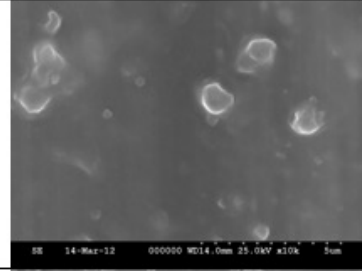
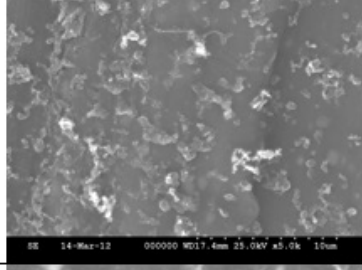
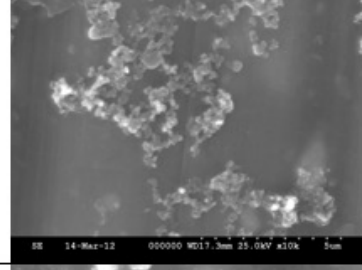
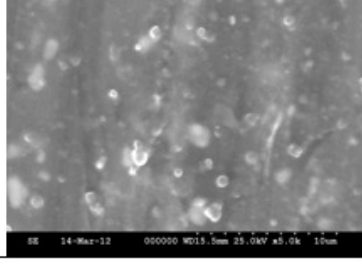
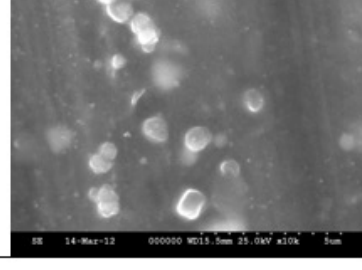
Run	Fuel	Temp/C	Particle coverage	Particle size (qualitative)	Particle Morphology	Image1 (5000X) 10µm	Image 2 (10,000X) 5µm
Run 13 Stub 2	25/75 TFE/Kapton	540°	Medium coverage over a film.	Most particles <2.2µm; much smaller particles >0.1µm.	Mostly spherical. Agglomerates typically composed of similarly sized particles.		
Run 18 & 38 Stub 2	25/75 TFE/Kapton	640°	Sparse	Particles generally ~0.2µm-3.5µm; most <1.1µm.	Particles appear larger and somewhat spherical, larger particles appear to consist of two different types of particles.		
Run 11 Stub 2	100% Kapton	540°	Extremely heavy	Particles range from ~0.1µm – 3.3µm, with most less than 0.5µm.	Most particles are spherical, some adhere to each other in strings.		
Run 16 Stub 2	100% Kapton	640°	Heavy	Most particles <1.0µm; including a significant population 0.3 µm and below.	Larger particles are agglomerates; some doublets and triplets.		

TABLE 1.—CONTINUED.

Run	Fuel	Temp/C	Particle coverage	Particle size (qualitative)	Particle Morphology	Image1 (5000X) 10µm	Image 2 (10,000X) 5µm
Run 2 (Sept)	Nomex	640°	Moderate	A few larger particles >4µm, with most spherical particles <0.5µm.	Most particles are spherical, with some crustal and some compact amorphous particles.		
Run 1 Stub 2	<u>Std Mix</u>	540°	Moderate	Up to ~5.5µm, most <0.2µm through 0.5µm.	Spherical, some appearing to be collapsed; some appear as coated agglomerates of smaller particles.		
Run 2 (ignited after initial <u>pyrolysis</u> ) Stub 2	<u>Std Mix</u>	540°	Heavy	Usually <1.0µm; most ~0.1-0.7µm.	Large loose agglomerates (from combustion [ignition of gases] after initial oxidative pyrolysis)		
Run 4 Stub 2	<u>Std Mix</u>	540°	Moderate	Generally <2.2µm; majority ~ 0.2-1.0µm.	Mostly spherical with larger particles consisting of agglomerated primary particles (<100nm).		

The construction of the FR-4 begins with a woven glass fabric (E-glass, an alumino-borosilicate glass (Baker et al. 2004)) which is impregnated with epoxy resin. Circuit boards can be plated with tin, gold, nickel or copper, and the circuit board fuel in these tests was granulated and included components (integrated circuits [IC] microcircuits attached to the board with tin-lead solder) which can contain many other materials: silicone encapsulant; aluminum, gold or copper wires; copper or nickel alloy leadframes, among others. Printed circuit boards and components thermally decompose at different rates, with IC components having higher thermal stability owing to the prominence of Si which enhances char formation (Duan and Li, 2010). The printed circuit board fuel used in the smoke tests is the composite material FR-4, which has been developed to be flame retardant (hence the abbreviation ‘FR’). Halogens are added to the glass-reinforced epoxy laminate to make the boards flame resistant, or self-extinguishing, and studies on thermal recycling of circuit board waste show that bromine is present as high as 8.5 weight percent (Chien et al. 2000).

In several tests, collection of printed circuit board smoke particles on an aluminum SEM stub in the thermal precipitator often resulted in a film layer with distinct embedded particles and clusters of particles as small as 150 nm to 200 nm, as seen in Figure 1.

Most particles observed on the SEM stub were somewhat spherical or compact agglomerates, however, the TEM grid analyses revealed other distinct types and features, including encapsulated and coated particles, char particles as well as crustal particles. Sheridan et al. (1994) defined the compositional category of crustal particles for atmospheric aerosols, to include O and at least two elements common in the Earth’s crust: Si, Al, Ca, and Fe. It has since become a common particle characterization category, with some authors including additional crustal elements (Ramirez-Leal et al. 2014, Li et al. 2011, Furutani et al. 2011, Mogo et al. 2005, Chen et al. 1998).

Figure 2 shows a limited number of particles in the left image (highlighted with arrows) with diameters on the order of 200 to 400 nm, and a detail of the particle (red box) in the right image (approximately 350 nm in diameter) with its corresponding EDS spectrum below. Note that in the EDS spectra shown, some Cu can be attributed to the copper TEM grid which supports the lacey carbon, although this peak is relatively large compared to other circuit board particles and it logically is expected to appear in the circuit board smoke particles from copper layers in the board or the clad laminate. Figure 2 has a prominent bromine peak, as well as Pb, which is also common in many circuit board smoke particles sampled with the thermal precipitator.

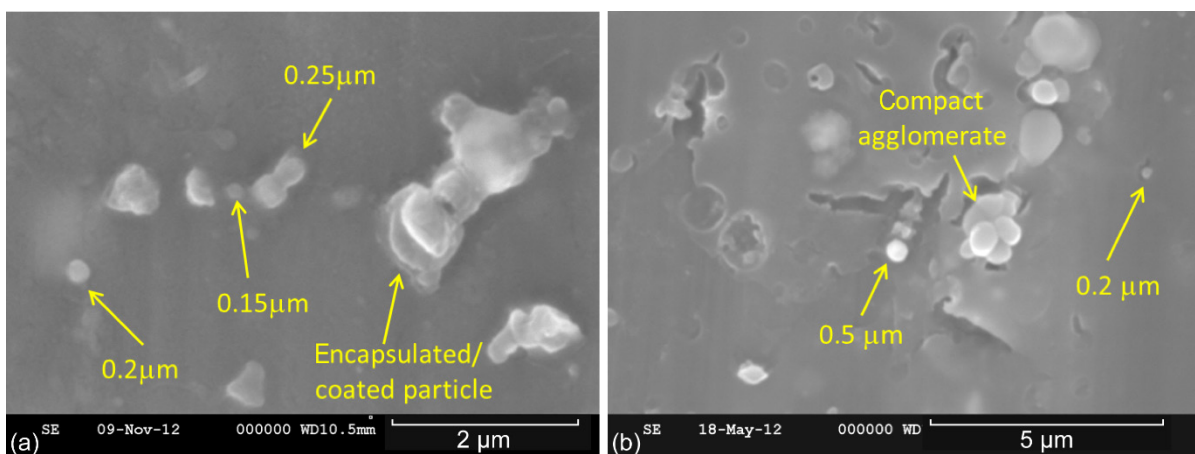


Figure 1.—SEM images of circuit board smoke particles. (a) At 640 °C (Run 33). (b) At 340 °C (Run 27).

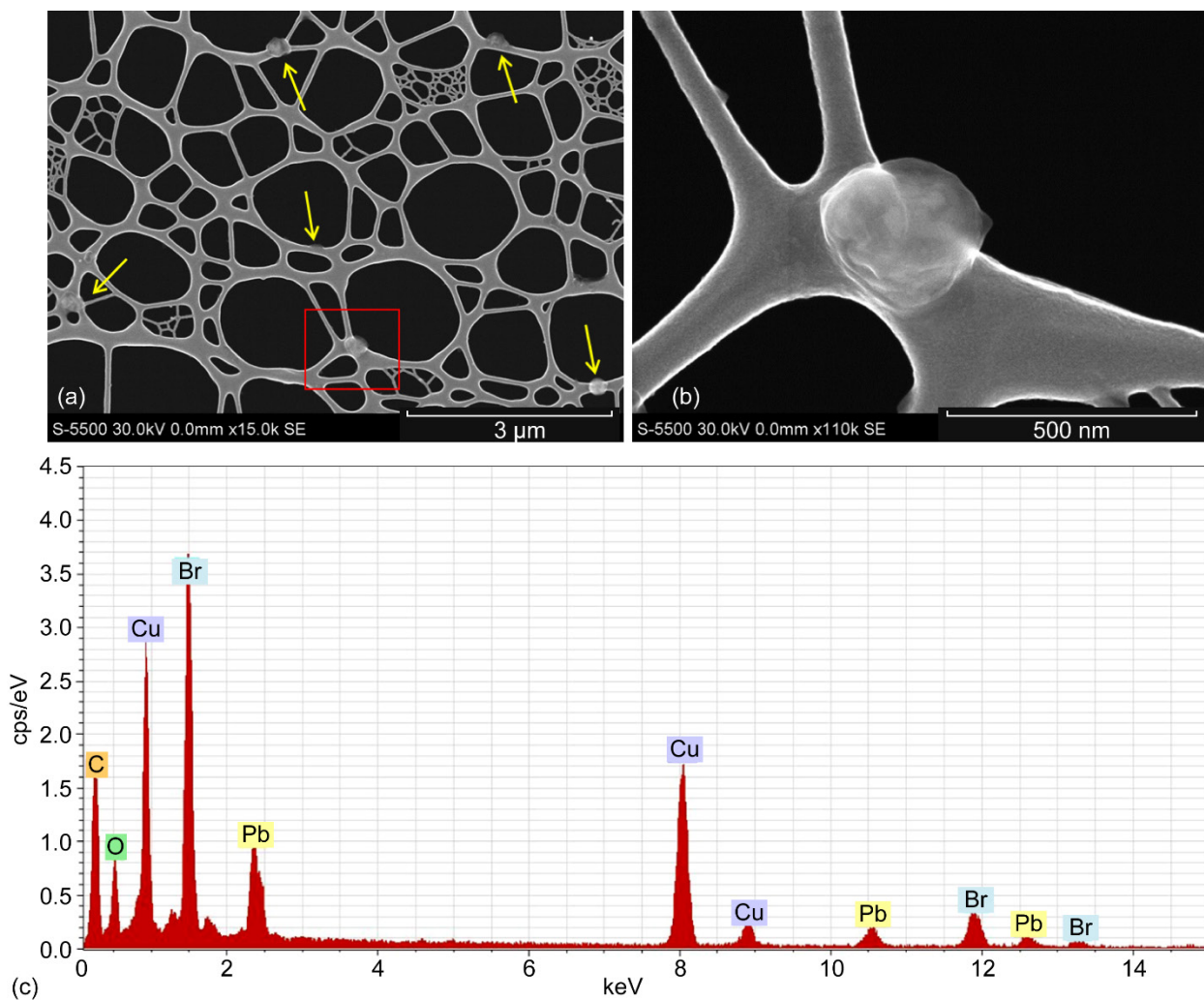


Figure 2.—Lacey carbon TEM grid with circuit board smoke particles at 540 °C (Run 31). (a) Typical rounded multi-component particles on the order of 200 to 400 nm diam. (b) Detail of particle in red box, approximately 350 nm diam. (c) Corresponding EDS spectrum showing Br, Cu, and Pb, which are typical constituents of circuit board and component materials. Cu can also be attributed to the TEM grid.

Figure 3 is an example of an irregular particle with inclusions (the particle is distinctly internally heterogeneous). The inclusions range from 40 to 60 nm, and some may be agglomerated to the surface, but most appear to be bound within the coating of the particle. Elements in the EDS spectrum include Cu, Br, Pb and Si. Cu can be attributed to the copper TEM grid which supports the lacey carbon grid and the Si signal may be attributed to the mica sheet in the smoke generator.

Figure 4 shows High resolution STEM (Hitachi HD-2300) images of inclusions in circuit board smoke particles, which demonstrate a Pb/Br-rich particle with a Br-rich coating, with Si often present in the coating as well. Note that the inclusions in the right image appear to be crystalline, with recognizable angular crystal faces.

Figure 5 is an image of a crustal particle along with its EDS spectrum showing a significant Si peak and a minor Al peak (both can be attributed to the E-glass in the circuit board, although the Al may be a system peak). Elements detected within circuit board smoke particles (including other EDS spectra not shown) are C, O, F, Fe, Cu, Al, and Si. Gases evolved from overheating circuit board include CO, HF, HCl and off-line ion chromatography analyses also show HBr from these tests (Meyer et al. 2013).

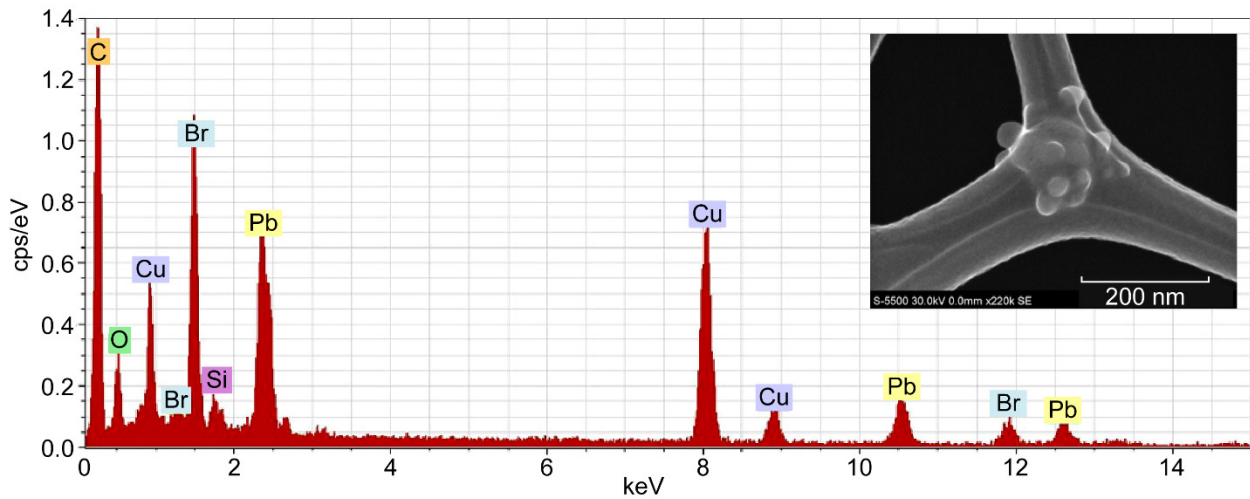


Figure 3.—EDS spectrum of a circuit board smoke particle at 540 °C with TEM grid image (inset) (Run 31).

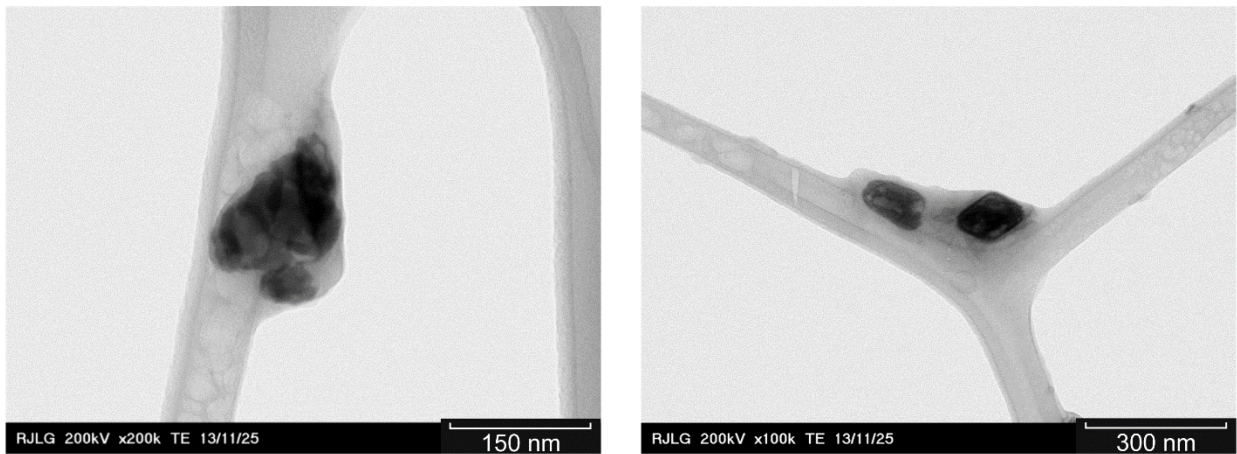


Figure 4.—High resolution STEM image details on inclusions within circuit board smoke particles at 540 °C (Run 31).

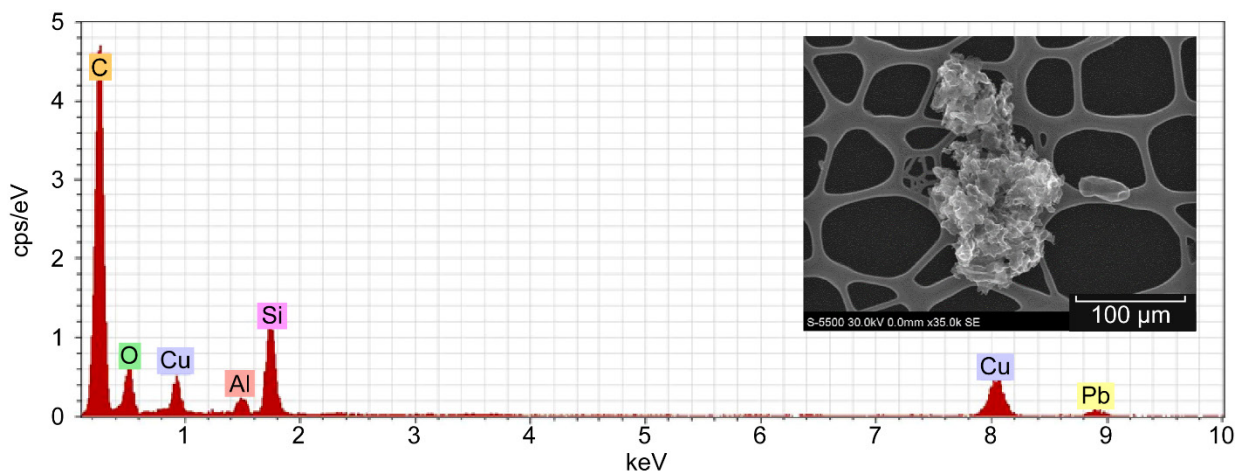


Figure 5.—EDS spectrum of circuit board smoke particle (inset) at 540 °C (Run 31) and TEM image. The jagged crystalline particle is much larger than the typical rounded particles and EDS shows a significant Si peak as well as Cu and Al, all typical constituents of electronics (circuit board and components).

## 4.0 Smoke Particles From Wire Insulation

Along with circuit boards, thermal degradation of wire insulation has high potential as a source of smoke in spacecraft. Samples of partially fluorinated polyimide (PFPI) wire insulation manufactured by TRW were overheated and smoke particles collected with the thermal precipitator. PFPI polymers were invented under NASA Lewis Research Center sponsorship in the late 1970s and were targeted as superior candidates for high temperature wire insulation products (Jones, 1994). This PFPI wire insulation was shown to generate smoke in previous testing within 35 sec at current levels from 10 to 15 A, and smoke reportedly vented from bubbles and imperfections in the insulation (Hammoud et al. 1995). Figure 6 shows two distinct PFPI smoke particle morphologies from thermal precipitator sampling, spherical and crystalline.

The majority of the wire insulation smoke particles captured are spherical, some appearing as doublets, as in the left image of Figure 6. Larger square and angular crystalline particles are less common, as shown in the center and right images of Figure 6.

Some notable yet infrequent large spherical particles were observed ranging in diameter from 4.0 to 4.6  $\mu\text{m}$ , as shown in Figure 7. These larger particles appear to have somewhat irregular surfaces which are most likely smaller particles agglomerating on the surface, as evident in the right image of Figure 7. The advantage of collecting SEM images is the ability to observe particle surface features and morphology with distinct details, including the 300 nm particle and other particles adhered to the sphere in the right image. Striations in the aluminum surface finish SEM stub are evident in the right image.

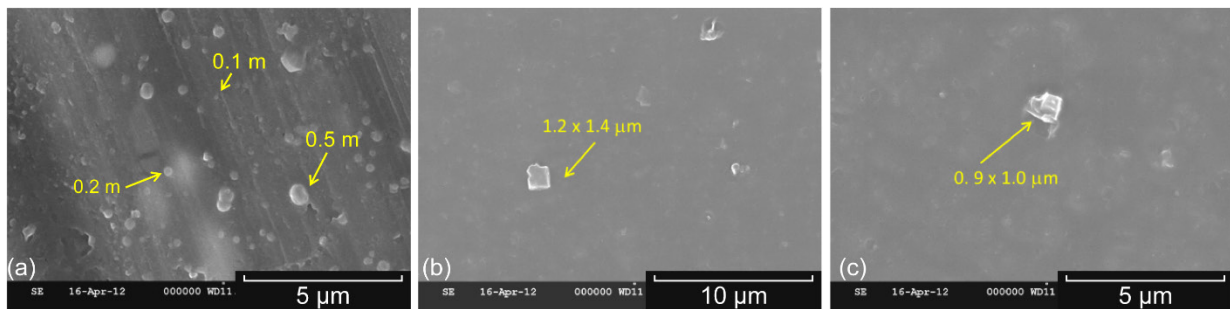


Figure 6.—SEM images of wire insulation smoke particles at 640 °C (Run 6). (a) Smaller particle populations are mostly spherical. (b) and (c) Particles with square crystalline morphology.

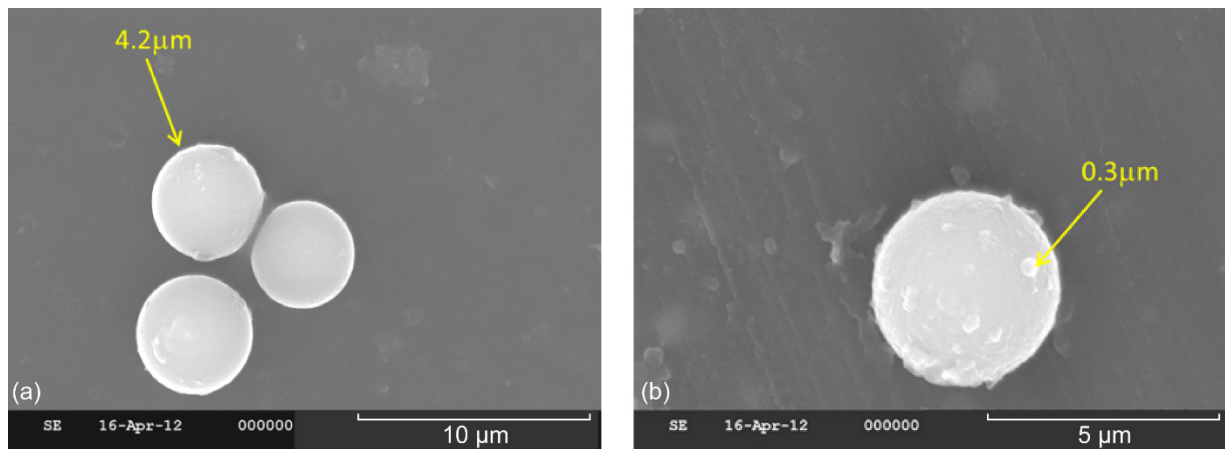


Figure 7.—SEM images of wire insulation smoke particles at 640 °C (Run 6). These large spheres range from 4.0 to 4.6  $\mu\text{m}$  diameter. (a) Three spherical particles in proximity. (b) Note the smaller particles adhered to the large particle.

## 5.0 Smoke Particles From Teflon

Teflon is the DuPont Company trade name of polytetrafluoroethylene (PTFE,  $(C_2F_4)_n$ ), a crystalline fluoropolymer commonly used in spacecraft for wire insulation, water storage bladders, sampling bags, suits, and cargo liners. The thermal decomposition of Teflon differs from the other polymers analyzed in spacecraft fire characterization testing. Teflon polymer fragments are released during the pyrolysis of Teflon, as opposed to polymers which release low and high molecular weight gases. These fragments, ejected under the same temperatures as the heating range of these tests, grow through nucleation, condensation and coagulation (Mulholland et al. 2015).

Teflon smoke particles collected with the thermal precipitator had nearly spherical morphology of varying sizes, as seen in Table 1. Figure 8 and Figure 9 show high resolution SEM images (Hitachi S-5500) of typical Teflon smoke particles which are nearly spherical. Although these particles are fairly large (typically greater than 500 nm), it is evident that many smaller particles have agglomerated to the surfaces, some as small as 50 nm in diameter.

Smoke particles in Figure 8 and Figure 9 were collected on two different types of TEM grids that were attached to carbon tape on the SEM stubs, one with continuous carbon film between the copper grid matrix, and the other with lacey carbon between the copper grid openings.

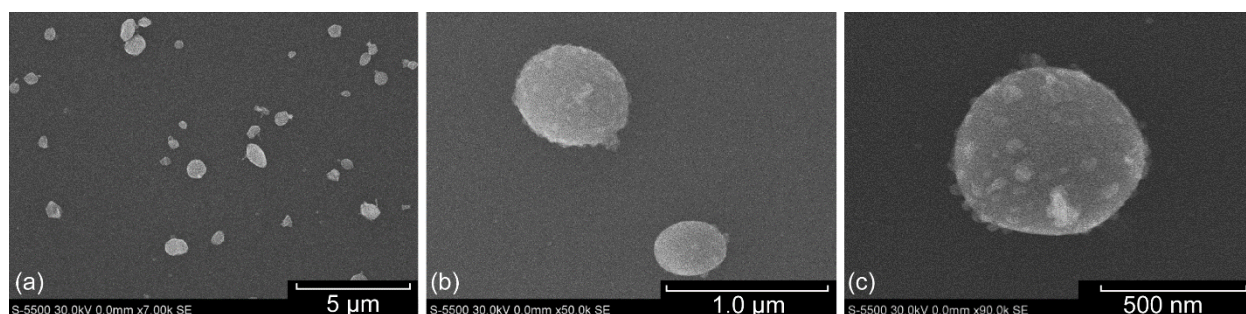


Figure 8.—High resolution SEM images of Teflon smoke particles at 540 °C collected onto a carbon film TEM grid. (a) 250 nm to 1.5 μm diam. range. (b) 500 nm and 700 nm diam. (c) 700 nm diam.

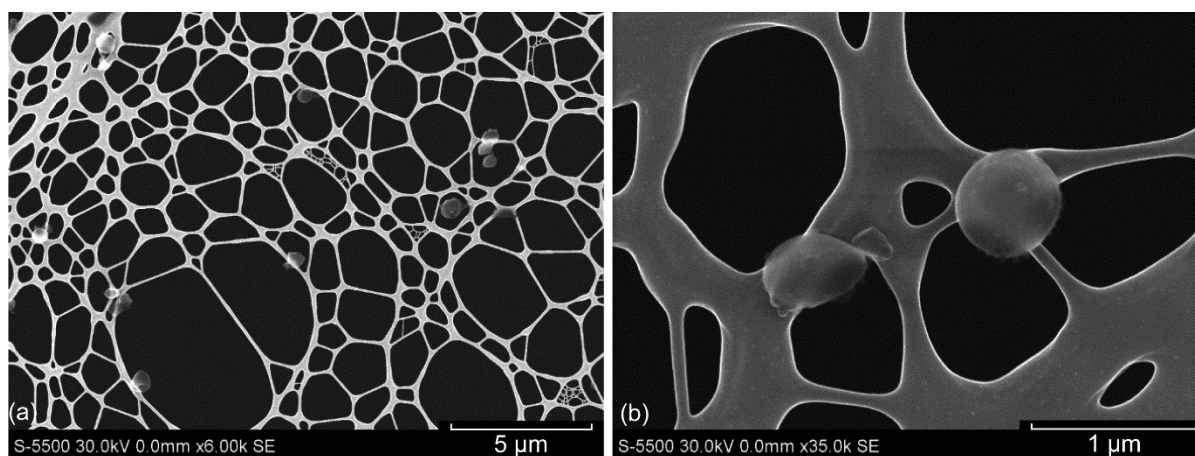


Figure 9.—High resolution SEM images of Teflon smoke particles at 540 °C collected onto a lacey carbon TEM grid. (a) Representative particles. (b) 700 nm and approximately 400 nm diam.

An EDS spectrum and image of a Teflon smoke particle are shown in Figure 10. The prominent fluorine peak is expected, and indicates that the material did not completely thermally decompose during heating, substantiating that intact fragments of polymers are liberated in the smoke.

However, the elements Al and Si are not expected to appear in Teflon smoke particles. The Al is most likely a system peak, Cu can be attributed to the copper TEM grid which supports the lacey carbon, and Si is potentially from the mica liner in the WSTF smoke generator.

Several typical Teflon smoke particles were examined at higher magnifications in a TEM (Philips Model CM20) in order to reveal some chemical information about the structure and order of the particle material. Figure 11 shows high resolution TEM images of a Teflon smoke particle (640 °C) approximately 400 nm in diameter adhered to the lacey carbon. The irregular rounded particle on the left appears to be composed of layers and/or agglomerated smaller particles, as seen by the varying density (darkness) and has a tail which is magnified in the center and right images. The particle tail is thinner than the particle itself and it is hanging over the edge of the lacey carbon support structure, which allows imaging of the microstructure. The center image shows smaller particles in the tail which have either agglomerated or become encapsulated. The far right image shows the amorphous interior structure of the tail.

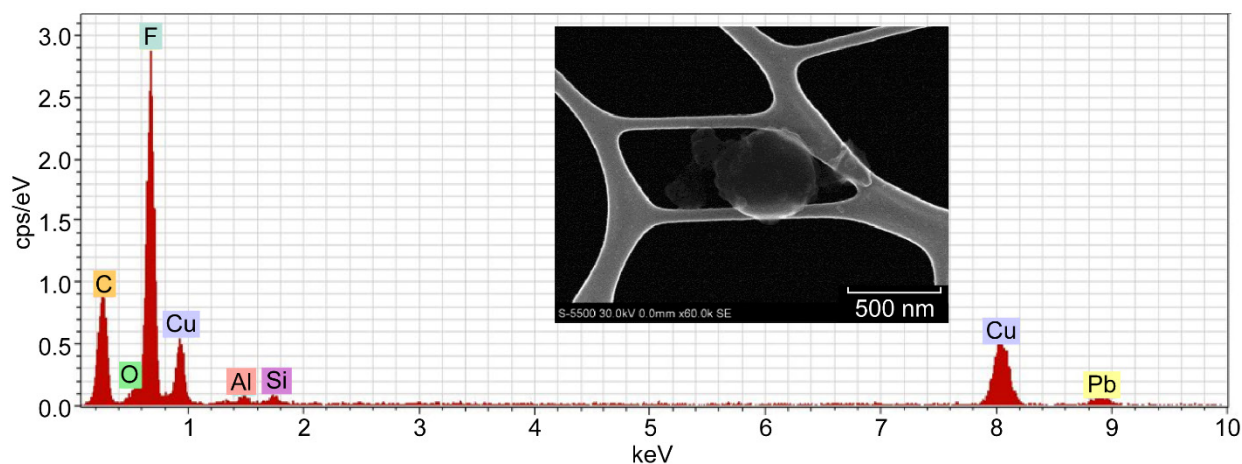


Figure 10.—High resolution SEM image of Teflon smoke particle (inset) at 540 °C collected on a lacey carbon TEM grid and corresponding EDS spectrum with a prominent F peak.

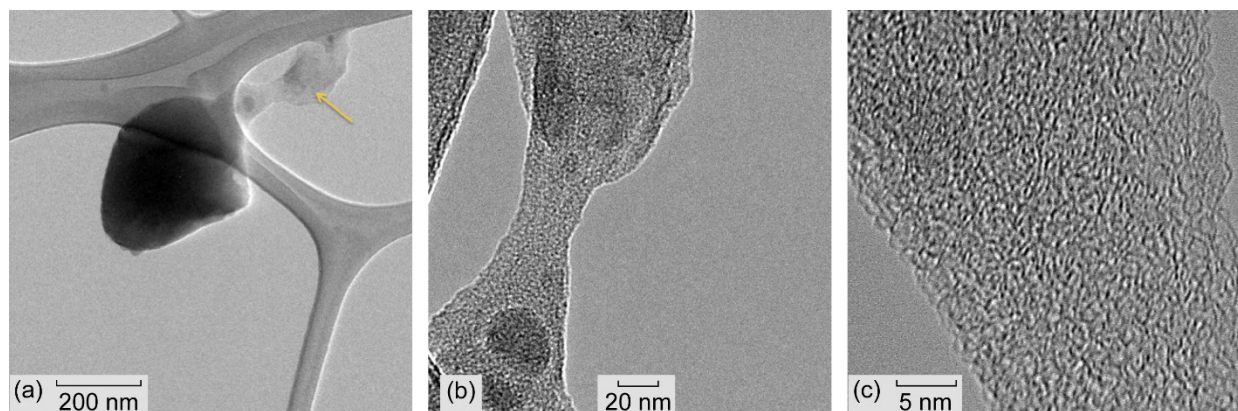


Figure 11.—High resolution TEM images of a Teflon smoke particle at 640 °C (test 15) adhered to a lacey carbon TEM grid. (a) The irregular rounded particle with an extended tail is approximately 400 nm in diameter. (b) Particle tail detail which contains smaller particles. (c) Amorphous interior structure of the tail.

Figure 12 shows a 250 nm spherical Teflon smoke particle, which appears to consist of many smaller particles bound together by amorphous material as seen in the right image of Figure 12, which is at higher magnification and interior particles are on the order of 20 to 30 nm. This primary particle size has been confirmed by initial particle size measurements of fresh smoke in the test chamber, however, within seconds, the extremely small particles rapidly combine into larger agglomerates in the high concentrations typically seen in the smoke chamber. Teflon particles are known to escape detection by photoelectric smoke detectors owing to their small size.

Figure 13 shows a portion of a much larger agglomerate with distinctly angular shaped protrusions. The center and right images are magnified portions of the angular agglomerate and the morphology shows evidence of crystallinity. This is not unexpected for Teflon, which can be up to 90 percent crystalline.

Images in Figure 14 are the highest magnification images which illustrate the individual carbon fringe structures or nanostructures of the agglomerate particle of Figure 13. The linear pattern in the interior of the particle shows the alignment of crystal fringes within an amorphous carbon coating. This substantiates that the original crystalline material fragments have persisted through the heating cycle and were subsequently coated by amorphous products condensing on the surface.

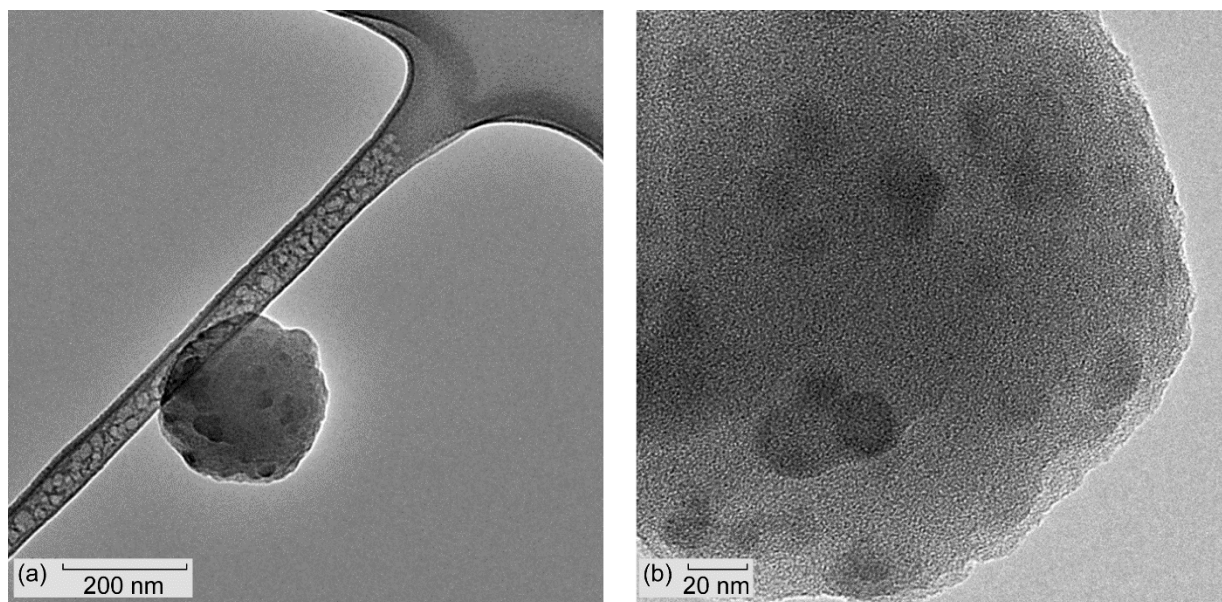


Figure 12.—High resolution TEM images of a Teflon smoke particle at 640 °C (test 15) adhered to a lacey carbon TEM grid. (a) Compact agglomerate, approximately 250 nm diam. contains smaller particles bound together by amorphous material. (b) Particle detail.

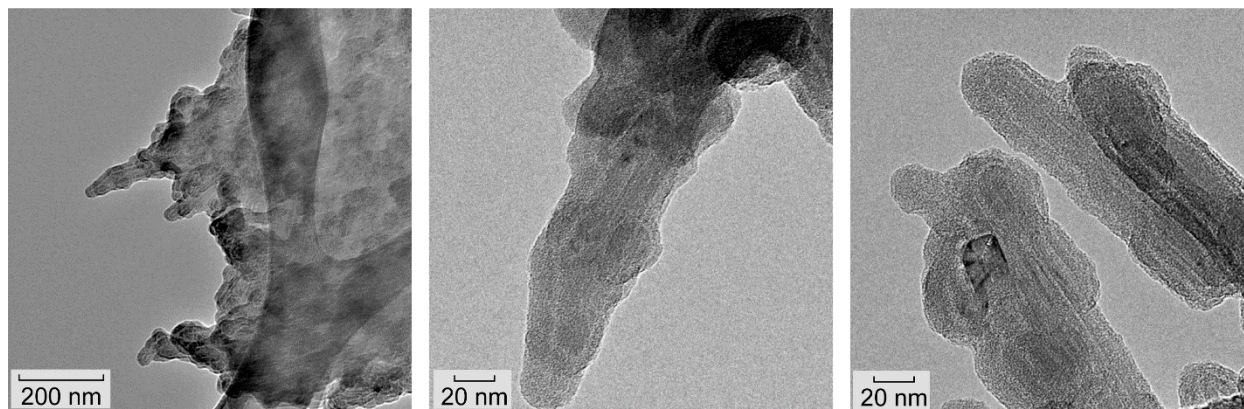


Figure 13.—High resolution TEM images of a Teflon smoke particle at 640 °C (test 15).

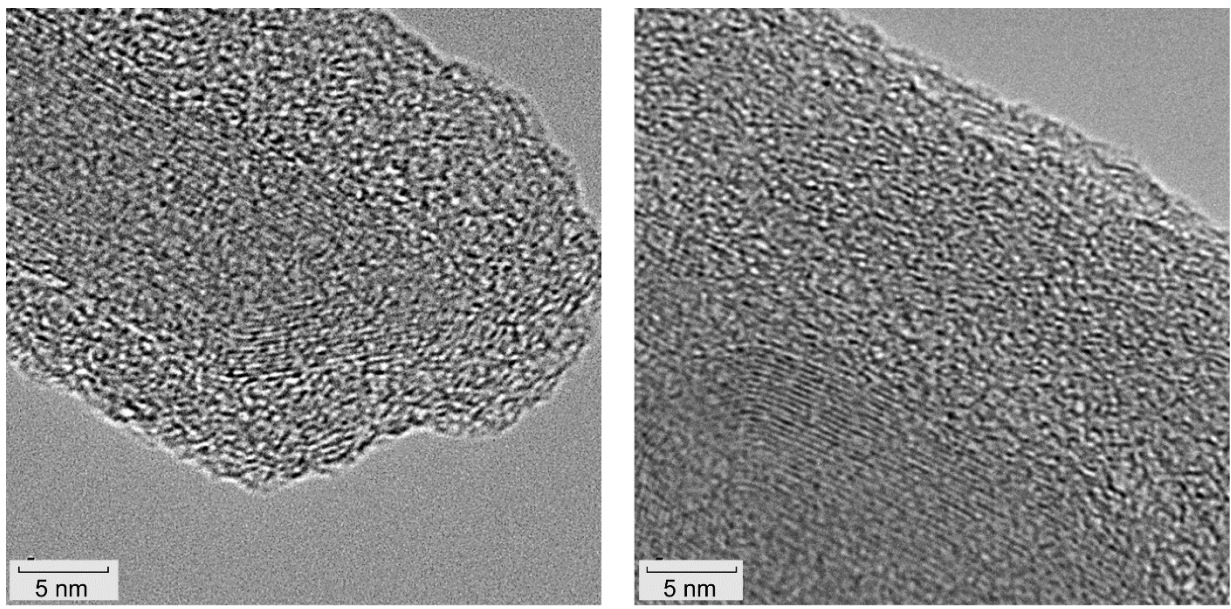


Figure 14.—High resolution TEM images of a Teflon smoke particle at 640 °C (test 15) showing a crystalline interior with an amorphous coating.

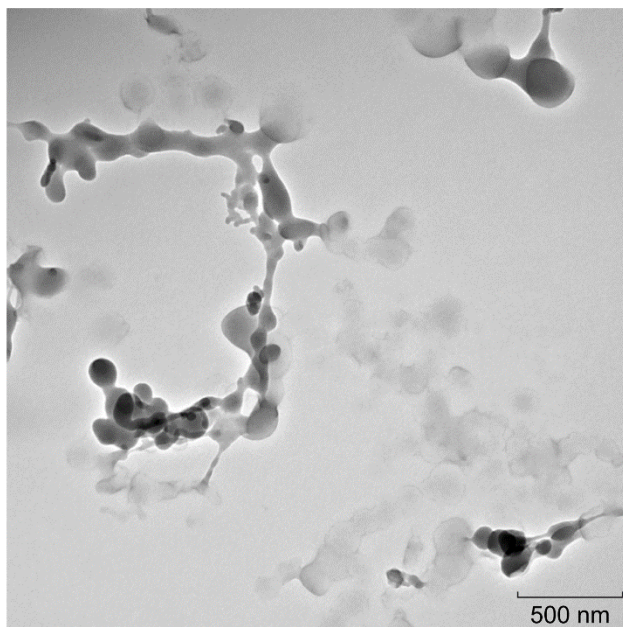


Figure 15.—Teflon smoke particles collected with the SAME thermal precipitator on the ISS, showing vastly different morphology compared to WSTF samples (TEM, Philips Model CM20).

Teflon smoke particles from the WSTF thermal precipitator are very different from the morphology observed in the NASA Smoke Aerosol Measurement Experiment (SAME), performed on the International Space Station (ISS), and pictured in Figure 15, most likely because of different heating methods and fuel preparation (Meyer et al. 2015).

## 6.0 Smoke Particles From Kapton

Kapton, a polyimide with chemical formula  $(C_{22}H_{10}N_2O_5)_n$  performs well at both high and low temperatures and has excellent insulating properties and fire resistance. Spacecraft applications of Kapton include thin-film heaters, wire insulation, space suits, tape and multi-layer insulation (MLI). Thermal decomposition of Kapton results in liquid aromatic products, and the general spherical shape of the particles observed with the TEM is consistent with the particles starting as a liquid solution with many components (Mulholland et al. 2015). Kapton smoke particles under heating conditions of these tests can form chain-like agglomerate structures.

Figure 16 shows SEM images of Kapton smoke particles generated at 540 °C (left image) which are either spherical or angular, ranging from 100 to 500 nm in diameter. The right image of Figure 16 shows particles generated at 640 °C in the same size range, which exhibit chain-like agglomerate structures and are coated by condensed pyrolysis products. These particles are on the aluminum SEM stub, and the striations in the unpolished surface are evident in the images.

Figure 17 shows high resolution SEM images of Kapton smoke particles on the lacey carbon TEM grid. These particles are in the same size ranges as the SEM images in Figure 16 although at higher magnification. Some particles appear to have angular edges and uneven surfaces. In the lower left image of Figure 17, the string of primary spherical particles ranging from 100 to 350 nm seem to be held together by liquid bridges that solidified.

Figure 18 shows an angular Kapton smoke particle 640 °C with its EDS spectrum with peaks for O, Si and Al. In all the spectra shown, Cu is attributed to the copper TEM grid which supports the lacey carbon, Al may be a system peak and the presence of Al and Si may be attributed to the mica liner in the WSTF smoke generator.

Figure 19(a) shows the coverage achieved with the thermal precipitator during a 640 °C test. The Cu grid around the carbon film appears on either side of the left image. The middle image shows a 450 nm spherical particle with a surface similar to previous particles, but with multiple smaller particles adhered to it. The right image of Figure 19 shows a chain of three particles all close to 350 nm in diameter, one irregularly shaped which is attached to two more spherical particles with rough surfaces, most likely from smaller agglomerated particles. Figure 20 shows a 400 nm Kapton smoke particle with a similar rough surface texture.

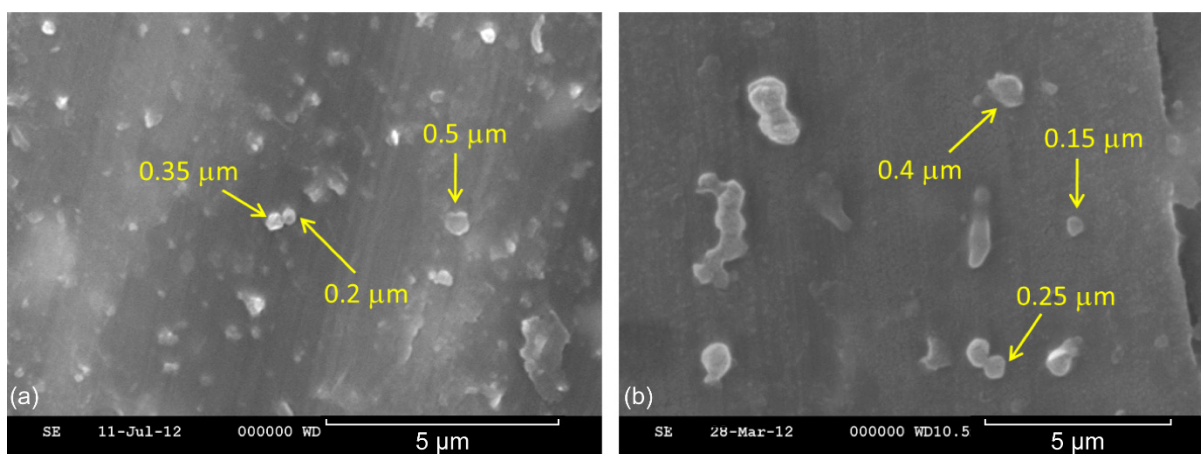


Figure 16.—SEM images of Kapton smoke particles on the Al SEM stub. (a) At 540 °C are compact and either spherical or angular. (b) At 640 °C exhibit chain-like agglomerate structures, some doublets and longer chains are coated.

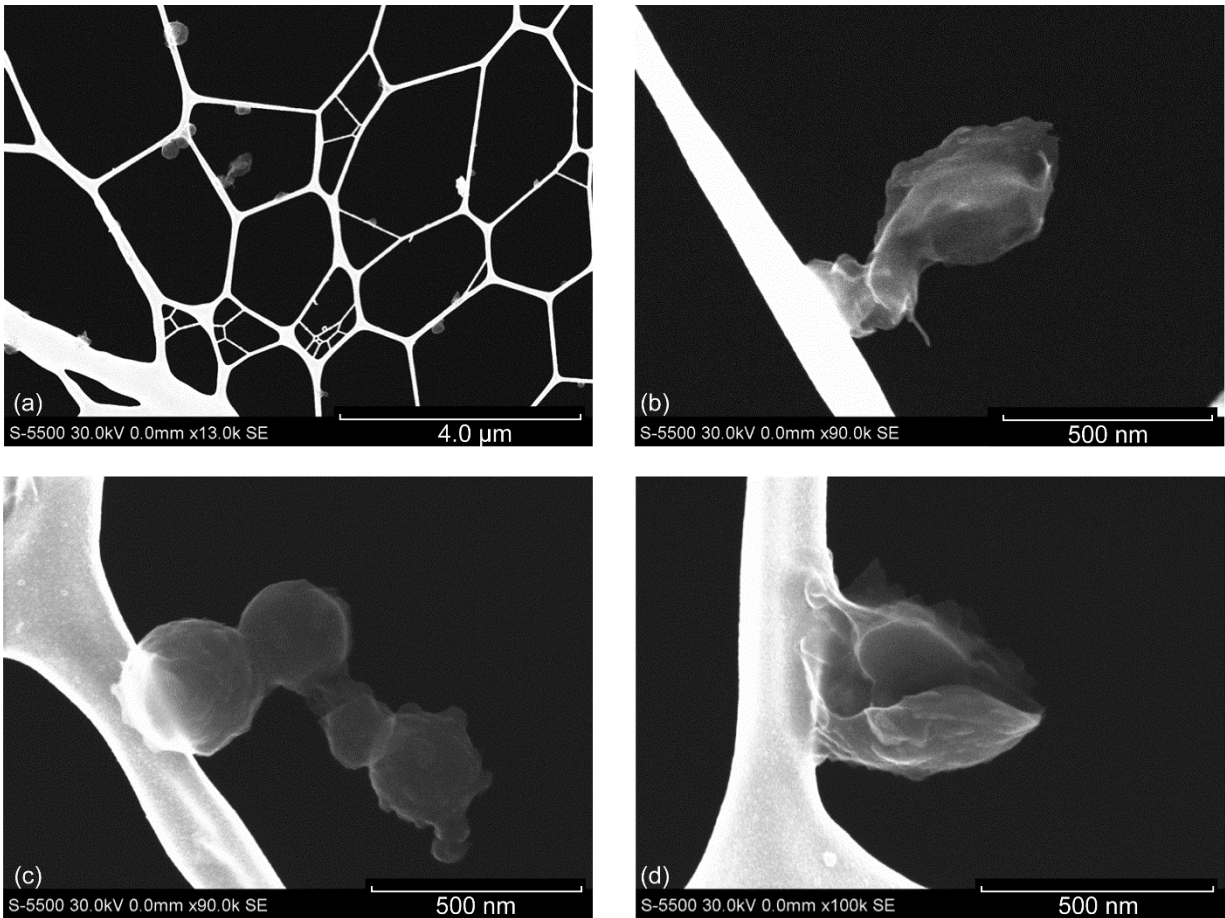


Figure 17.—High resolution SEM analysis of Kapton smoke particles at 640 °C on a lacey carbon TEM grid showing irregular surfaces and angular edges. (a) Typical coverage. (b) Approximately 700 nm long. (c) The coating on spherical particle chain appears to have primaries connected by liquid bridges that solidified and connected primary particles ranging from 100 to 350 nm. (d) 500 nm particle.

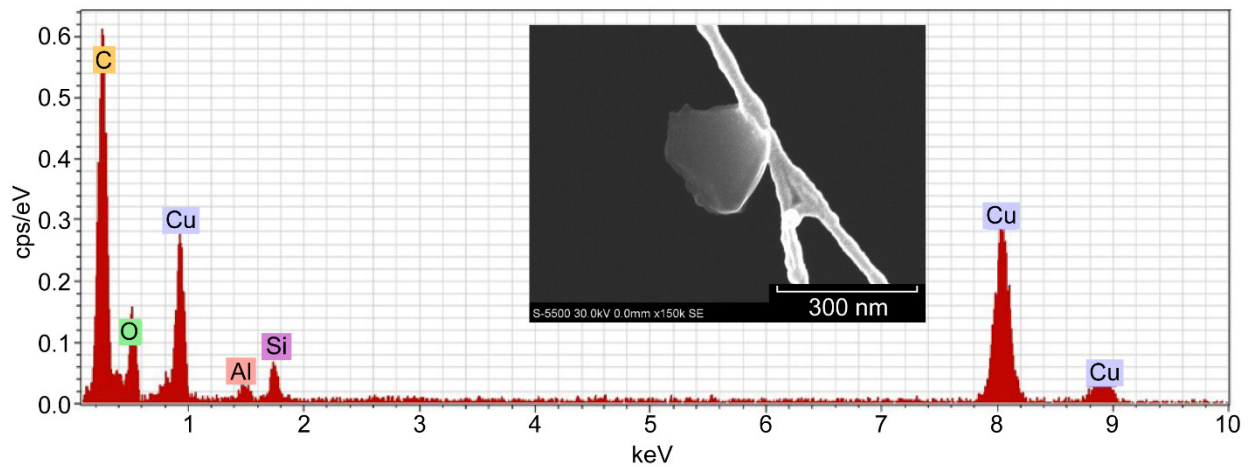


Figure 18.—Angular Kapton smoke particle (inset), approximately 270 nm at 640 °C with its EDS spectrum showing O, Si, and Al. The Al is most likely a system peak, Cu can be attributed to the copper TEM grid, and Si is potentially from the mica liner in the WSTF smoke generator.

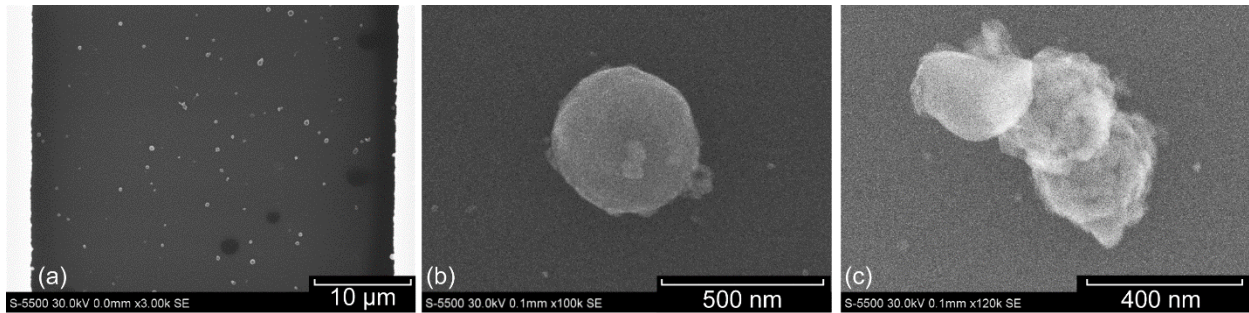


Figure 19.—High resolution SEM images of Kapton smoke particles at 640 °C. (a) Typical coverage. (b) 450 nm spherical particle with multiple smaller particles adhered to it. (c) Chain of three particles all close to 350 nm diam.

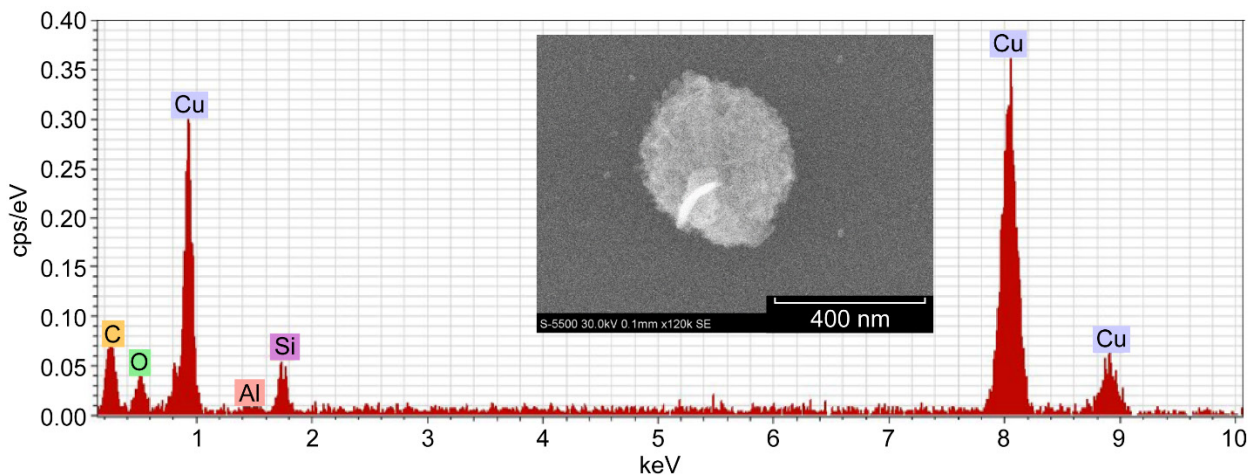


Figure 20.—EDS spectrum of a 400 nm Kapton smoke particle (inset) at 640 °C on a carbon film TEM grid showing Cu, Si, and Al. The Al is most likely a system peak, Cu can be attributed to the copper TEM grid and Si is potentially from the mica liner in the WSTF smoke generator.

Both the compact irregular Kapton smoke particle in Figure 18 and the more spherical particle with a textured surface in Figure 20 contain the same elements, although the former has a higher C peak. The Al is most likely a system peak, Cu can be attributed to the copper TEM grid and Si is potentially from the mica liner in the WSTF smoke generator. Kapton smoke particles shown here compare well to the morphology observed in the NASA Smoke Aerosol Measurement Experiment (SAME), in spite of very different heating methods and fuel preparation (Meyer et al. 2015). Figure 21 shows aged Kapton particles collected with the SAME thermal precipitator on the ISS, which have similar spherical morphology and connected as doublets, triplets and longer chains and some appearing to have a somewhat rough surface. Furthermore, all the diameters of single particles shown in the WSTF micrographs are within the ranges of the smoke particle size distributions measured with the Scanning Mobility Particle Sizer Spectrometer (SMPS) in the ground testing of SAME flight hardware heating Kapton and the size distribution obtained from image analysis (projected area equivalent diameter) of pyrolysis smoke particles collected on a TEM grid on board the ISS.

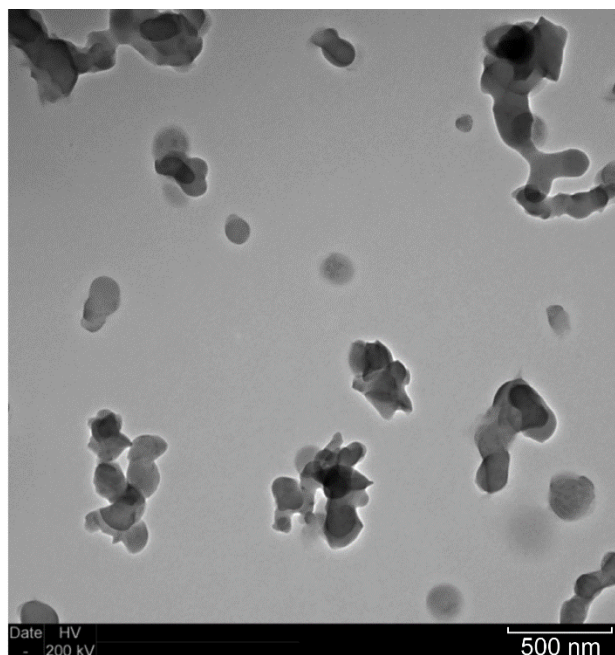


Figure 21.—Aged Kapton smoke particles collected with the SAME thermal precipitator on the ISS showing similar morphology to WSTF samples (TEM, Philips Model CM20).

## 7.0 Smoke Particles From Nomex

Nomex cloth is a heat and flame-resistant textile woven from continuous meta-aramid polymer fibers (DuPont chemical company). It is an aromatic polyamide produced by condensation reaction from two monomers, m-phenylenediamine and isophthaloyl chloride (Chanda and Roy, 2008). In spacecraft applications, Nomex cloth is used for acoustic insulation, cargo bags, thermal blankets and pressure suits.

Nomex affords a longer heat-resistance owing to carbonization during thermal decomposition (Vilar-Rodil et al. 2001). Zhang (2010) performed analysis of the thermal degradation of Nomex fibers using TGA-DTA/FT-IR (Thermogravimetric analysis—differential thermal analysis/Fourier Transform—Infrared) and reported that above 500 °C, complex depolymerization, random rupture, restructuring and other chemical reactions take place. As the Nomex is heated without combustion (oxidative pyrolysis), many organic species are liberated leaving a carbon-rich ash or char.

Nomex smoke particles were observed with four types of morphology: irregular char-like, irregular with inorganics, rounded irregular and spherical. Figure 22 shows the Nomex smoke particles on the aluminum SEM stub, with many spherical particles, some irregular rounded particles, and one large crustal particle in addition to several other smaller irregular crustal particles.

Figure 23 shows what appear to be a char particles as the accompanying EDS spectra show very large carbon peaks. In all the spectra shown, Cu is attributed to the copper TEM grid which supports the lacey carbon. The upper spectrum shows the presence of Al which is a system peak and Si is potentially from the mica liner in the WSTF smoke generator.

Figure 24 shows an irregular Nomex smoke particle with the EDS spectrum showing a large oxygen peak along with the inorganic elements Mg, Ca and Si, which appears larger than other system peaks.

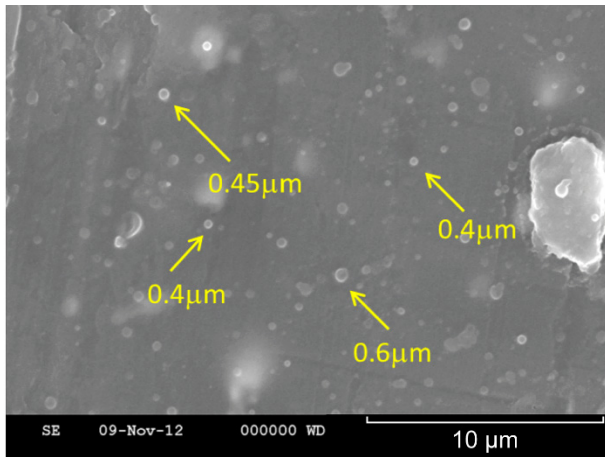


Figure 22.—SEM image showing spherical Nomex smoke particles in the 300 to 600 nm range and a large irregular particle (on the right), possibly char. Light areas indicate charging by the electron beam, however, the spherical particles are stable and did not volatilize under the beam.

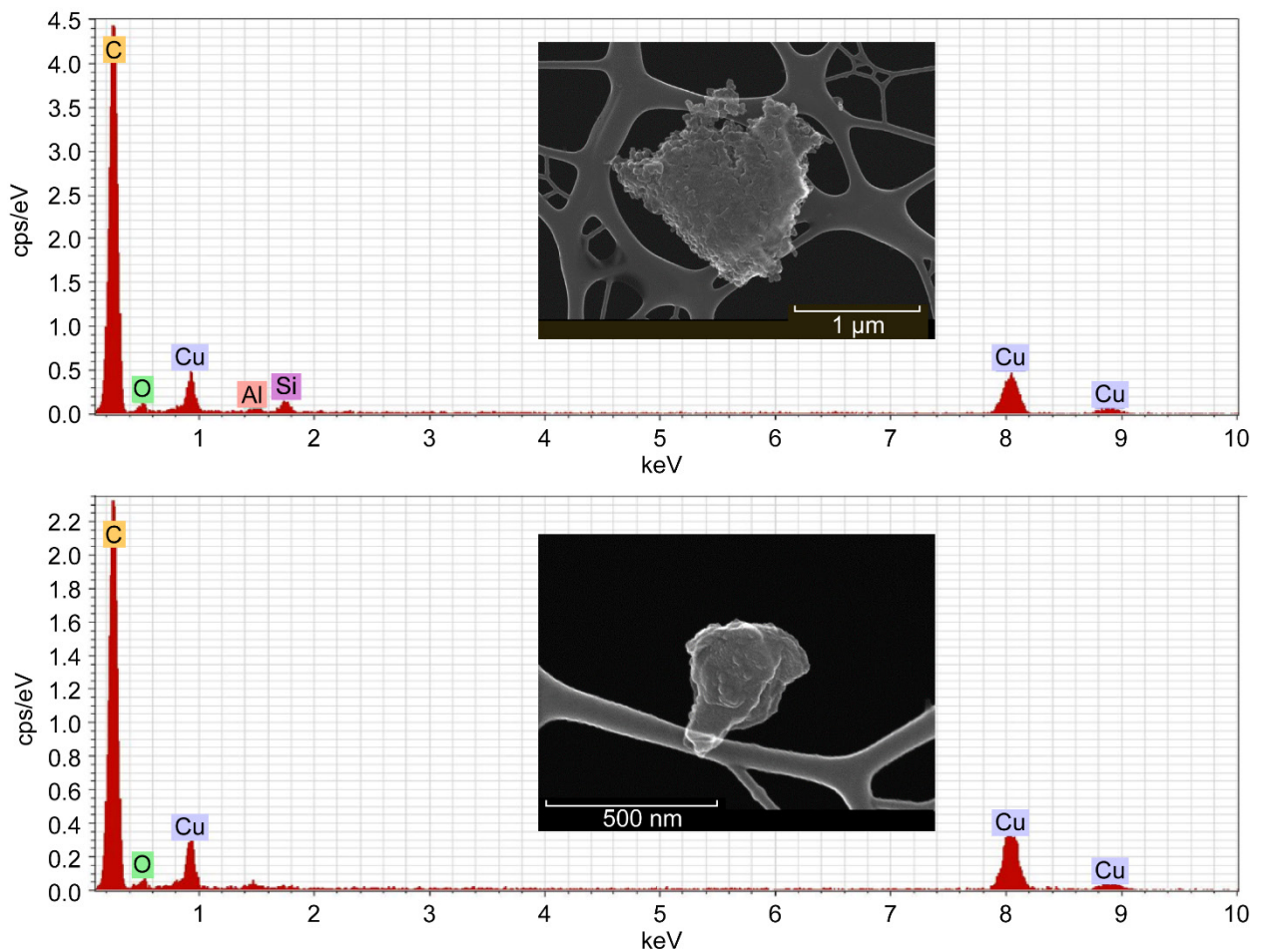


Figure 23.—SEM images and corresponding spectra from Nomex smoke of what appear to be char particles owing to the high C peaks. Cu in both spectra are attributed to the copper TEM grid in the upper spectrum.

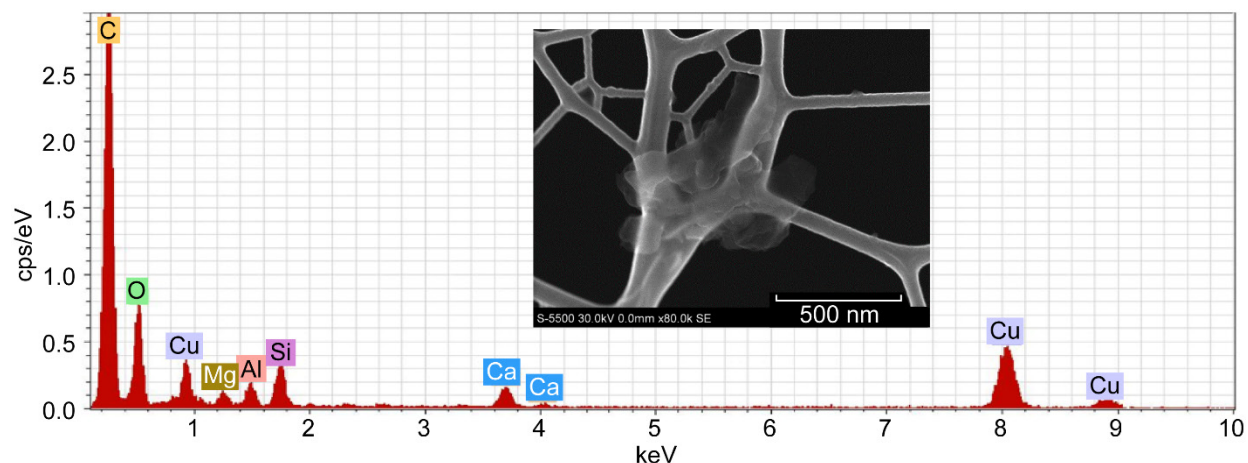


Figure 24.—Spectrum of an irregular Nomex smoke particle with distinct angular inclusions (inset), containing O as well as the elements, Si, Ca, Al, and Mg. The Al may be a system peak and Cu can be attributed to the copper TEM grid.

Figure 25 is an irregular rounded Nomex smoke particle that is amorphous, and appears to have arrived at the TEM grid in a partially-solidified viscous liquid state. The EDS spectrum shows the particle contains C, O, N, Al, Si and Cl. The presence of Cl in the Nomex smoke particles is explained by the polymer formation process which uses a condensation reaction with isophthaloyl chloride, and furthermore, the reaction is catalyzed with LiCl, and the solution used in spinning Nomex fibers typically contains more than 3 percent calcium chloride ( $\text{CaCl}_2$ ) by weight (Fink, 2008, Gabara et al. 2006). The Nomex used for fuel in these tests emits HCl gas in WSTF and GASP (Gases & Aerosols from Smoldering Polymers) laboratory testing at levels ranging from 20 to 115 ppm, depending on the fuel mass, while HCN and HF are also emitted in lesser concentrations (Briggs et al. 2015, Meyer et al. 2013).

The process of carbonization during Nomex pyrolysis can be seen as a parallel to the carbonization taking place in making charcoal and to biomass burning in general, as well as to coal pyrolysis. Tar has been generally defined in the literature as any condensable product emitted from the heating of solid fuel (Bond and Bergstrom 2006). More specifically, in coal combustion research, it is referred to as aromatic cluster fragments with lower molecular weights (Wang et al. 2013, Wang et al. 2015). In the biomass combustion/pyrolysis literature, tar is referred to as high-molecular weight water-insoluble organic polymer species, and a liquid from biomass distillation products (Hand et al. 2005, Tóth et al. 2014, Fang et al. 2014). The definition of tar with regards to thermal decomposition of organic materials (coal, biomass and polymers) is of importance in the classification of particles as ‘tar balls’. Tar balls have been observed in wildfire emissions as well as laboratory generated smoldering and combustion, in both fresh and aged smoke (Pósfai et al. 2003, Li et al. 2003, Pósfai et al. 2004, Tivanski et al. 2007, Chakrabarty et al. 2010, Turmolva et al. 2010, Adachi and Buseck, 2011, China et al. 2013, Tóth et al. 2014). Characteristic descriptions of tar balls in the above-mentioned literature vary somewhat, depending on the smoke source sampled and analyzed, but most include the following traits: carbonaceous, perfectly spherical to near-spherical, amorphous and with homogeneous composition (without inorganic inclusions, crystalline structure, graphene microstructures or internal cores). Tar balls are stable/resistant to electron beam damage under high magnification and are classified optically into two types: dark and bright, based on degree of oxidation and coating. Their absorption Ångström coefficients indicate they can be categorized as brown carbon, which is a type of organic carbon that is brownish or yellowish in appearance and has an imaginary refractive index that varies with wavelength (Moosmüller et al. 2009). Tar ball EDS spectra reportedly consist of C, N, O, (some sources include inorganic species S, Cl, K and

Si as well) and have a high C/O atomic ratio. Tar balls appear externally mixed, that is, they do not agglomerate with other particle types. They are reportedly produced from smoldering combustion, nucleated from the gas phase within smoke plumes (gas to particle formation mechanism), and vary based on environmental conditions: fuel type, formation temperature and transport/aging in the atmosphere (Pósfai et al. 2003, Li et al. 2003, Pósfai et al. 2004, Tivanski et al. 2007, Chakrabarty et al. 2010, Turmolva et al. 2010, Adachi and Buseck, 2011, China et al. 2013, Tóth et al. 2014).

Tóth et al. (2014) created the first laboratory-generated tar ball particles by droplet emissions of liquid tar obtained by dry distillation of wood. After aerosolization of the liquid, the tar droplets had a residence time of about 0.3 sec in a heated zone between 560 and 630 °C which solidified the droplets into particles with all the characteristics of tar balls. They hypothesize that tar balls may be formed by expulsion of liquid tar from biomass pores upon pyrolysis which are solidified by a short residence time in the flame zone of a fire.

The thermal decomposition of Nomex creates liquid smoke particles, so surface tension dictates the final shape. Some particles arrive at the TEM grid mostly solidified, as spheres, while some adhere to the lacey carbon grid before solidifying, as seen in Figure 26.

The temperatures used in the generation of tar balls from liquid tar by Tóth et al. (2014) are similar to the conditions of the Nomex heating test (640 °C). Nomex smoke samples collected with the thermal precipitator had some perfectly spherical particles which have a striking resemblance to tar balls, and it can be assumed that the tar droplets had long enough residence time in the heated zone of the smoke generating tube furnace to solidify, however, there are a number of particles that were clearly liquid when they were captured on the TEM grid.

Figure 27 shows a tar ball-like Nomex smoke particle which is attached to the lacey carbon by a small liquid bridge. The EDX spectrum shows the elements C, N, O, as reported in tar ball descriptions in the literature, but also the presence of Al, which is a system peak from the specimen holder. All the magnified smoke particles in Figure 26 have the same elements in their EDX spectra as the one shown in Figure 27 (C, N, O and Al), and the upper right image has Cl in its spectrum as well.

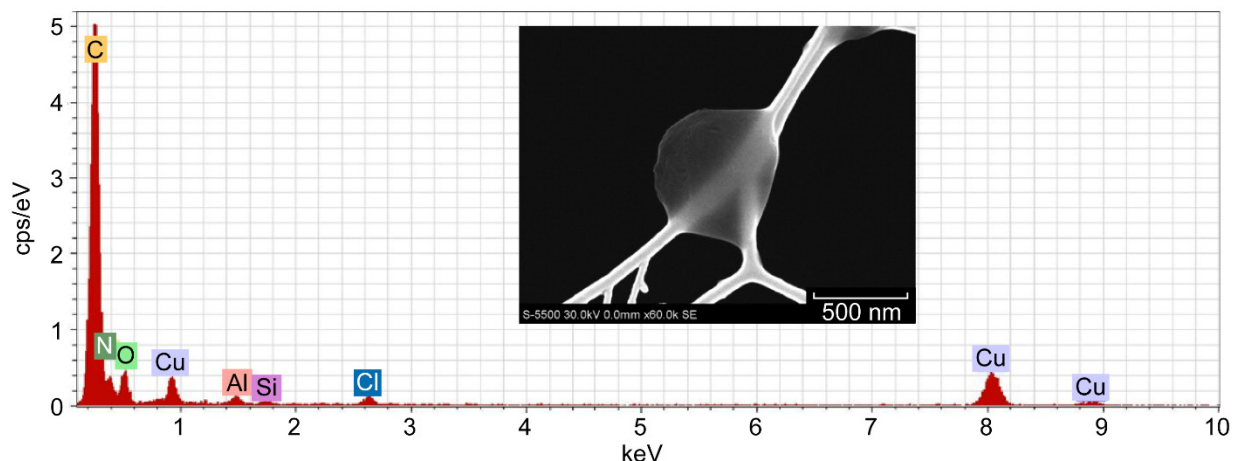


Figure 25.—EDS spectrum of a non-spherical 700 nm Nomex smoke particle with a rounded irregular shape (inset) containing C, O, N, Al, Si, and Cl. The Al may be a system peak, Cu can be attributed to the copper TEM grid and Si is potentially from the mica liner in the WSTF smoke generator.

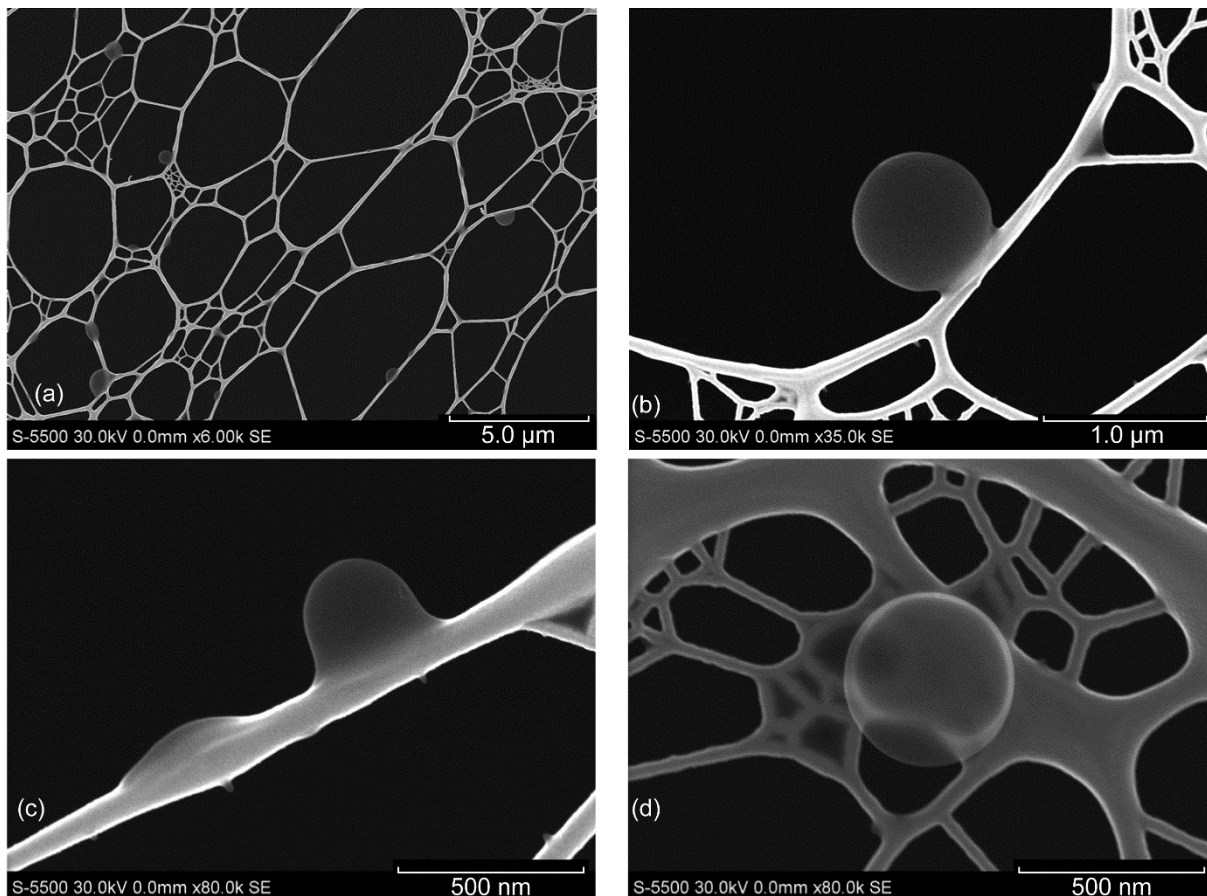


Figure 26.—High resolution SEM images of Nomex smoke particles that appear on the TEM grid as liquid droplets of varying solidity, some with perfectly spherical tar ball morphology. Diameters of single particles range from 300 to 800 nm. (a) Large scale image showing coverage (b) 800 nm. (c) 300 nm. (d) 450 nm.

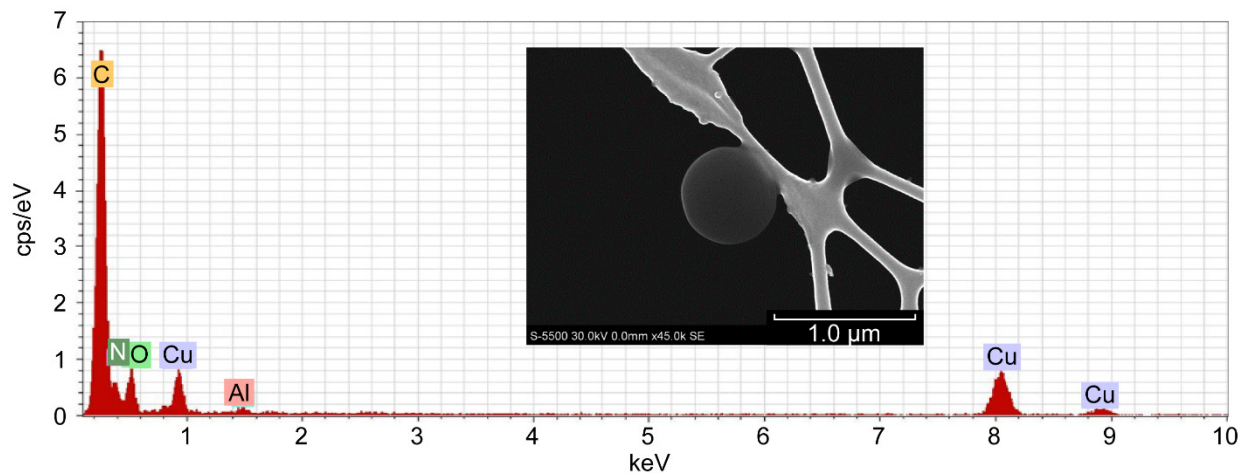


Figure 27.—EDS spectrum of a tar ball-like 600 nm Nomex smoke particle (inset) with peaks of C, O, N, Al, Si, and Cl.



Figure 28.—Nomex fuel tests. (a) Nomex snips before heating (0.5 g fuel sample). (b) After heating, the Nomex snips became one or two compact pieces of char/ash, as shown in the remains of five different tests. (c) TEOM filters after mass concentration measurements of Nomex smoke particles show the characteristic yellowish color of brown carbon.

Figure 28 shows the Nomex fuel before and after heating. The left image shows 0.5 g of the fluffy unburned fabric, randomly snipped into pieces 1 cm or less per side. The fuel undergoes carbonization in the furnace, reducing the small pieces of fibrous Nomex to individual clumps of char as the fibers thicken and combine when subjected to intense heat (Nomex Technical Guide, 2001), as seen in the center image of Figure 28. A Tapered Element Oscillating Microbalance (TEOM) was used as a reference instrument for mass concentration in these experiments. This instrument uses consumable filters which must be replaced when the instrument pressure drop becomes too high. Upon removal, most TEOM filters from other polymer fuels were barely discolored (mostly white), with the exception of PVC smoke, which was very dark brown, nearly black. Another notable exception was Nomex smoke which made the TEOM filters yellowish brown, the color typically observed for brown carbon. The used TEOM filters from the WSTF testing in which these particles were collected are shown in Figure 28(c). This is additional evidence to support the hypothesis that Nomex smoke from oxidative pyrolysis includes tar balls.

## 8.0 Conclusions

The thermal precipitator successfully collected an abundance of smoke particles for microscopic analysis. A comprehensive characterization has been performed for each material, although there are many additional sampled particles which have not been examined. From the analyses to date, the following general conclusions are made:

- Ten types of common spacecraft materials or mixed materials underwent oxidative pyrolysis at different temperatures and the resulting smoke particles were characterized according to morphology and elemental composition.
- Results are consistent with known thermal decomposition mechanisms in the literature and chemical make-up of spacecraft fuels.
- Teflon particles show evidence of native polymer shards liberated from the bulk material based on elemental mapping and high resolution TEM micrographs showing a crystalline interior with an amorphous coating.
- Under the heating conditions of these tests, Teflon particles coagulate into compact spherical agglomerates, unlike SAME Teflon smoke particles which were fractal agglomerates in both ground testing and ISS tests.

- Kapton smoke particles are consistent in size and morphology with SAME smoke from ISS experiments and ground testing.
- Crustal particles, rich in inorganic species, were observed in circuit card smoke.
- Tar ball morphology was observed for Nomex smoke particles.

Ongoing spacecraft smoke characterization research takes place in GASP (Gases & Aerosols from Smoldering Polymers) laboratory at the NASA Glenn Research Center. Current experiments focus on quantifying smoke aerosol and acid gas concentrations generated with these and other spacecraft fuels.

## References

- Adachi, K.; and Buseck, P.R.: Atmospheric Tar Balls From Biomass Burning in Mexico. *J. Geophys. Res.*, vol. 116, D05204, 2011.
- Baker, A.; Dutton, S.; and Kelly, D.: Fibers for Polymer-Matrix Composites. *Composite Materials for Aircraft Structures*. Second ed., ch. 3, AIAA, Reston, VA, 2004.
- Briggs, R., et al.: Qualification of a Multi-Channel Infrared Laser Absorption Spectrometer for Monitoring CO, HCl, HCN, HF, and CO<sub>2</sub> Aboard Manned Spacecraft. ICES–2015–300, 2015.
- Chakrabarty, R.K., et al.: Brown Carbon in Tar Balls From Smoldering Biomass Combustion. *Atmos. Chem. Phys.*, vol. 10, 2010, pp. 6363–6370.
- Chanda, M.; and Roy, S.K.: *Industrial Polymers, Specialty Polymers, and Their Applications*. *Plastics Engineering Series*, CRC Press, Boca Raton, 2008, pp. 1–80.
- Chen, Y., et al.: Single Particle Analyses of Ice Nucleating Aerosols in the Upper Troposphere and Lower Stratosphere. *Geophys. Res. Lett.*, vol. 25, no. 9, 1998, pp. 1391–1394.
- Chien, Y.C., et al.: Fate of Bromine in Pyrolysis of Printed Circuit Board Wastes. *Chemosphere*, vol. 40, issue 4, 2000, pp. 383–387.
- China, S., et al.: Morphology and Mixing State of Individual Freshly Emitted Wildfire Carbonaceous Particles. *Nature Comm.*, vol. 4, article no. 2122, 2013.
- Duan, H.; and Li, J.: Thermal Degradation Behavior of Waste Video Cards Using Thermogravimetric Analysis and Pyrolysis Gas Chromatography/Mass Spectrometry Techniques. *J. Air Waste Manag. Assoc.*, vol. 60, 2010, pp. 540–547.
- DuPont Technical Guide for NOMEX<sup>®</sup> Brand Fiber. H–52720, DuPont Advanced Fibers Systems, Richmond, VA, 2001.
- Durlak, S.K., et al.: Characterization of Polycyclic Aromatic Hydrocarbon Particulate and Gaseous Emissions From Polystyrene Combustion. *Environ. Sci. Technol.*, vol. 32, no. 15, 1998, p. 2301.
- Fang, J.; Leavey, A.; and Biswas, P.: Controlled Studies on Aerosol Formation During Biomass Pyrolysis in a Flat Flame Reactor. *Fuel*, vol. 116, 2014, pp. 350–357.
- Fink, Johannes Karl: *High Performance Polymers*. Ch. 13, William Andrew Inc., New York, 2008.
- Furutani, H., et al.: Single-Particle Chemical Characterization and Source Apportionment of Iron-Containing Atmospheric Aerosols in Asian Outflow. *J. Geophys. Res.*, vol. 116, D18204, 2011.
- Gabara, V., et al.: *Handbook of Fiber Chemistry*. *International Fiber Science and Technology Series*, Lewin, M., ed., Third ed., ch. 13, CRC Press, Boca Raton, FL, 2006, p. 1001.
- Hammoud, A.N., et al.: Performance of Partially Fluorinated Polyimide Insulation for Aerospace Applications. NASA Contractor Report 198372, 1995. <http://ntrs.nasa.gov/>
- Hand, J.L., et al.: Optical, Physical, and Chemical Properties of Tar Balls Observed During the Yosemite Aerosol Characterization Study. *J. Geophys. Res.*, vol. 110, D21210, 2005.

- Jones, R.J.: High Temperature Polymer Dielectric Film Insulation. NASA Technical Reports Server TRW-N94-28715 (SAE Technical Paper 941187), 1994. <http://ntrs.nasa.gov/>
- Lambert, R.: The Impact of Materials on the Flammability of Printed Wiring Board Products. Proceedings of the 43rd Electronic Components and Technology Conference, 1993, pp. 134-142.
- Li, W.J., et al.: Individual Particle Analysis of Aerosols Collected Under Haze and Non-haze Conditions at a High-Elevation Mountain Site in the North China Plain. *Atmos. Chem. Phys.*, vol. 11, 2011, pp. 11733-11744.
- Meyer, M.E., Design of a Thermal Precipitator for the Characterization of Smoke Particles From Common Spacecraft Materials, NASA/TM—2015-218746, June 2015.
- Meyer, M.E., et al.: Materials Combustion Testing and Combustion Product Sensor Evaluations in FY12. Proceedings of the 43rd International Conference on Environmental Systems (AIAA 2013-3432), Vail, CO, 2013.
- Meyer, M.E., et al.: Smoke Characterization and Feasibility of the Moment Method for Spacecraft Fire Detection. *Aerosol Sci. Tech.*, vol. 49, no. 5, 2015, pp. 299-309.
- Mogo, S.; Cachorro, V.E.; and de Frutos, A.M.: Morphological, Chemical and Optical Absorbing Characterization of Aerosols in the Urban Atmosphere of Valladolid. *Atmos. Chem. Phys.*, vol. 5, 2005, pp. 2739-2748.
- Moosmüller, H.; Chakrabarty, R.K.; and Arnott, W.P.: Aerosol Light Absorption and Its Measurement: A Review. *J. Quant. Spectrosc. Radiat. Transfer*, vol. 110, 2009, pp. 844-878.
- Mulholland, G.W., et al.: Pyrolysis Smoke Generated Under Low-Gravity Conditions. *Aerosol Sci. Tech.*, vol. 49, no. 5, 2015, pp. 310-321.
- Pósfai, M., et al.: Atmospheric Tar Balls: Particles From Biomass and Biofuel Burning. *J. Geophys. Res.*, vol. 109, D06213, 2004.
- Pósfai, M., et al.: Individual Aerosol Particles From Biomass Burning in Southern Africa: 1. Compositions and Size Distributions of Carbonaceous Particles. *J. Geophys. Res.*, vol. 108, issue D13, 8483, 2003.
- Ramirez-Leal, R.; Valle-Martinez, M.; and Cruz-Campas, M.: Chemical and Morphological Study of PM10 Analysed by SEM-EDS. *Open Journal of Air Pollution*, vol. 3, 2014, pp. 121-129.
- Sheridan, P.J.; Brock, C.A.; and Wilson, J.C.: Aerosol Particles in the Upper Troposphere and Lower Stratosphere: Elemental Composition and Morphology of Individual Particles in Northern Midlatitudes. *Geophys. Res. Lett.*, vol. 21, no. 23, 1994, pp. 2587-2590.
- Tivanski, A.V., et al.: Oxygenated Interface on Biomass Burn Tar Balls Determined By Single Particle Scanning Transmission X-ray Microscopy. *J. Phys. Chem. A*, vol. 111, 2007, pp. 5448-5458.
- Tóth, A., et al.: Atmospheric Tar Balls: Aged Primary Droplets From Biomass Burning? *Atmos. Chem. Phys.*, vol. 14, 2014, pp. 6669-6675.
- Tumulva, L., et al.: Morphological and Elemental Classification of Freshly Emitted Soot Particles and Atmospheric Ultrafine Particles Using the TEM/EDX. *Aerosol Sci. Tech.*, vol. 44, 2010, pp. 202-215.
- Villar-Rodil, S., et al.: Atomic Force Microscopy and Infrared Spectroscopy Studies of the Thermal Degradation of Nomex Aramid Fibers. *Chem. Mater.*, vol. 13, no. 11, 2001, pp. 4297-4304.
- Wang, X., et al.: Relationship Between Pyrolysis Products and Organic Aerosols Formed During Coal Combustion. Proceedings of the Combustion Institute, vol. 35, no. 2, 2015, pp. 2347-2354.
- Wang, X., et al.: Characterization of Organic Aerosol Produced During Pulverized Coal Combustion in a Drop Tube Furnace. *Atmos. Chem. Phys.*, vol. 13, 2013, pp. 10919-10932.
- Zhang, H.T.: Comparison and Analysis of Thermal Degradation Process of Aramid Fibers (Kevlar 49 and Nomex), *JFBI*, vol. 3, no. 3, 2010.





